10.1161/CIRCULATIONAHA.116.024270

Dipeptidyl Peptidase-4 Induces Aortic Valve Calcification by Inhibiting Insulin-like Growth Factor-1 Signaling in Valvular Interstitial Cells

Running Title: *Choi et al.; DPP4 as a Potential Therapeutic Target for CAVD*

Bongkun Choi, PhD[1]; Sahmin Lee, MD, PhD[2]; Sang-Min Kim, MS[1]; Eun-Jin Lee, PhD[1]; Sun Ro Lee, BS[1]; Dae-Hee Kim, MD, PhD[2]; Jeong Yoon Jang, MD[2]; Sang-Wook Kang, PhD[1]; Ki-Up Lee, MD[3]; Eun-Ju Chang, PhD[1]; Jae-Kwan Song, MD, PhD[2]

[1]Department of Biomedical Sciences, Asan Medical Center, Research Institute for Valvular Heart Disease, University of Ulsan College of Medicine, Seoul, Korea; [2]Division of Cardiology, Asan Medical Center, Research Institute for Valvular Heart Disease, University of Ulsan College of Medicine, Seoul, Korea; [3]Division of Endocrinology and Metabolism, Department of Internal Medicine, Asan Medical Center, University of Ulsan College of Medicine, Seoul, Korea

The first two authors contributed equally to this work.

Address for Correspondence:

Jae-Kwan Song, MD, PhD
Division of Cardiology, Asan Medical Center
Research Institute for Valvular Heart Disease
University of Ulsan College of Medicine
88 Olympic-ro 43 Gil, Songpa-gu
Seoul 05505, South Korea
Tel: +82-2-3010-3155
Fax: +82-2-486-5918
E-mail: jksong@amc.seoul.kr

Eun-Ju Chang, PhD
Department of Biomedical Sciences
Asan Medical Center
Research Institute for Valvular Heart Disease
University of Ulsan College of Medicine
88 Olympic-ro 43 Gil, Songpa-gu
Seoul 05505, South Korea
Tel: +82-2-3010-4262
Fax: +82-2-3010-5307
E-mail: ejchang@amc.seoul.kr

Journal Subject Terms: Animal Models of Human Disease; Basic Science Research; Cell Biology/Structural Biology; Mechanisms; Pathophysiology

Abstract

***Background*—**Calcification of the aortic valve leads to increased leaflet stiffness, and consequently to the development of calcific aortic valve disease (CAVD); however, the underlying molecular and cellular mechanisms of calcification remain unclear. Here, we identified that dipeptidyl peptidase-4 (DPP-4, also known as CD26) increases valvular calcification and promotes CAVD progression.

***Methods*—**We obtained the aortic valve tissues from humans and murine models (wild type and *eNOS*$^{-/-}$ mice), and cultured the valvular interstitial cells (VICs) and valvular endothelial cells (VECs) from the cusps. We induced osteogenic differentiation in the primary cultured VICs and examined the effects of the DPP-4 inhibitor on the osteogenic changes *in vitro* and aortic valve calcification in *eNOS*$^{-/-}$ mice. We also induced calcific aortic stenosis in male New Zealand rabbits (weight, 2.5–3.0 kg) via a cholesterol-enriched diet+vitamin D2 (25,000 IU, daily). Echocardiography was performed to assess the aortic valve area, and the maximal and mean trans-aortic pressure gradients at baseline and at 3-week intervals thereafter. After 12 weeks, we harvested the heart and evaluated the aortic valve tissue using immunohistochemistry.

***Results*—**We found that nitric oxide depletion in human VECs activates NF-κB in human VICs. Consequently, the NF-κB promotes DPP-4 expression, which then induces the osteogenic differentiation of VICs by limiting autocrine insulin-like growth factor-1 (IGF-1) signaling. The inhibition of DPP-4 enzymatic activity blocked the osteogenic changes in VICs *in vitro* and reduced the aortic valve calcification *in vivo* in a mouse model. Sitagliptin administration in a rabbit CAVD model led to significant improvements in the rate of change in aortic valve area, transaortic peak velocity, and maximal and mean pressure gradients over 12 weeks. Immunohistochemistry staining confirmed the therapeutic effect of Sitagliptin in terms of reducing the calcium deposits in the rabbit aortic valve cusps. In rabbits receiving Sitagliptin, the plasma IGF-1 levels were significantly increased, in line with DPP-4 inhibition.

***Conclusions*—** DPP-4-dependent IGF-1 inhibition in VICs contributes to aortic valve calcification, suggesting that DPP-4 could serve as a potential therapeutic target to inhibit CAVD progression.

Key-Words: aortic stenosis; aortic valve calcification; insulin-like growth factor-1; Dipeptidyl Peptidase-4, Valvular interstitial cell

Clinical Perspective

What is new?

- Reciprocal interactions between valvular endothelial cells and interstitial cells (VICs) are critical for development of calcific aortic valve disease (CAVD), but its molecular mechanisms remain elusive.
- We revealed previously unidentified roles of dipeptidyl pedtidase-4 (DPP-4) and insulin-like growth factor-1 (IGF-1) as key proteins of valvular calcification process and crucial targets for protecting CAVD development.
- Endothelial dysfunction increased the DPP-4 expression and promoter binding in aortic VICs with increased degradation of IGF-1 resulting in osteogenic differentiation of VICs.
- Treatment with a DPP-4 inhibitor was protective against the progression of aortic valve calcification in animal models of CAVD.

What are the clinical implications?

- We elucidated the mechanisms underlying the deleterious effects of endothelium-dependent activation of DPP-4 activity in inducing IGF-1 deficiency, leading to valvular calcification and development of CAVD.
- The DPP-4–IGF-1 axis is a promising therapeutic target considering favorable evidences supporting potential role of DPP-4 inhibitors in animal experiments and their availability in the current clinical practice.
- For successful drug repositioning of DPP-4 inhibitors, further studies are necessary to determine optimal dose and timing of medical intervention to prevent CAVD progression.

Introduction

Calcific aortic valve disease (CAVD) is characterized by valvular calcification, followed by aortic stenosis and subsequent heart failure.[1, 2] CAVD progression is accompanied by highly regulated biological changes, including fibrous thickening and osteogenic changes in the aortic valve,[3-6] wherein inflammation is the initiating event.[3, 4, 7] Although CAVD shares similar pathological features with atherosclerosis in terms of lipid deposition and inflammation,[7] previous trials with cholesterol-lowering statin therapy failed to prevent CAVD progression.[8, 9] Recent investigations identified reciprocal interactions between valvular endothelial cells (VECs) and valvular interstitial cells (VICs), which are critical for osteogenic changes in aortic valve tissues.[1, 4, 10, 11] However, the molecular mechanisms or targets for nonsurgical treatments, to prevent or slow the progression of CAVD, remain elusive.[12]

Dipeptidyl peptidase-4 (DPP-4, also known as CD26)—a multifunctional enzyme—is found in the catalytically active soluble form in plasma and on the surface of most cell types.[13, 14] DPP-4 cleaves the N-terminal dipeptides, i.e., proline or alanine residues, from its substrates. Because most DPP-4 substrates are incretin hormones, DPP-4 has become a major target for the treatment of type 2 diabetes mellitus; accordingly, the prescription of DPP4-inhibitors, a new class of oral hypoglycemics, has markedly increased over the past few years.[15, 16] Nevertheless, DPP-4 has a wide range of biologic functions, and can bind with numerous peptides that serve as potential substrates for DPP-4. The non-glycemic actions of DPP-4 and its inhibitor, particularly in cardiovascular disease involving the myocardium or heart valves, have not been fully characterized, and further studies are required.

In the present study, we assessed whether DPP-4 can serve as a molecular therapeutic target for aortic valve calcification. DPP-4 increases valvular calcification and promotes CAVD

progression by limiting autocrine insulin-like growth factor-1 (IGF-1) signaling via the enzymatic degradation of IGF-1 in human VICs and inducing the subsequent osteogenic transdifferentiation of these cells to calcifying cells. In particular, we aimed to demonstrate that the DPP-4–IGF-1 axis is an important mechanism to explain the reciprocal interactions between VECs and VICs, which play a critical role in valve homeostasis, and that this axis can be an effective therapeutic target for the prevention of CAVD progression.

Methods

Human Subjects

Human aortic valve tissues were obtained from patients with CAVD who underwent aortic valve replacement (n=10) and from extracted recipient hearts for use as non-CAVD controls (n=8) (Supplementary Table 1). Half of each sample specimen was used to prepare VECs and VICs, or was immediately stored in RNAlater (Life Technologies), whereas the other half was fixed in OCT compound (Sakura Finetek). The Institutional Review Board (IRB) of Asan Medical Center (Seoul, Korea) approved the study protocol for the collection of human samples (reference No. 2013-0442) and all patients provided written informed consent.

Animal Experiments

Mice

All animal experiments were performed according to the protocols approved by the Institutional Committee for the Use and Care of Laboratory animals. *eNOS*$^{-/-}$ mice with a C57BL/6 background were obtained from Jackson Laboratories. Wild-type (WT) and *eNOS*$^{-/-}$ mice (8 weeks of age) were randomly assigned and administered saline or Sitagliptin (15 mg/kg/day, Selleckchem) orally for 12 weeks. Mice were maintained on a 12 h light−dark cycle. Under

anesthesia, the mice were perfused with phosphate-buffered saline (PBS), followed by 4% buffered paraformaldehyde. Mice were euthanized, and blood and aortic valve samples were collected for analysis. The hearts were dissected, fixed overnight, and paraffin embedded. Serial sections (5 μm) were cut from the entire aortic valve area.

Rabbits

Twenty-nine male New Zealand white rabbits (weight, 2.5–3.0 kg) were used in this study. They were divided into 3 groups based on the diet and were followed for 12 weeks: 1) rabbits fed normal chow (control group, n=5); 2) rabbits fed 0.5% cholesterol-enriched chow (Dytes Inc.) plus 25,000 IU/day vitamin D2 (Vit.D2, Santa Cruz Biotechnology) in drinking water (Chol+Vit.D2 group, n=9); and 3) rabbits fed high cholesterol diet+vitamin D supplements and also administered Sitagliptin orally for 12 weeks (Sitagliptin group, n=15). Rabbits in the Sitagliptin group were again randomized according to the Sitagliptin dose: 4, 8, or 15 mg/kg/day. Blood samples were obtained via the marginal vein of the rabbit ear at baseline, and every 3 weeks thereafter. After 12 weeks, the rabbits were euthanized, and blood and aortic valve tissue samples were collected for analysis.

Statistical Analysis

All quantitative experiments were performed in triplicate (at a minimum). Data are presented as means±standard deviation. The Osteosense imaging and enzyme-linked immunosorbent assays (ELISAs) were performed by individuals blinded to the allocation during outcome assessment. *In vitro* data were normally distributed, with similar variances between the groups. Because of the small number of animals in each group and because some of the distributions were not normal in the animal study, a nonparametric analysis of variance was used to compare continuous variables between the groups. A two-tailed Student's *t*-test or nonparametric Kruskal-Wallis, Mann-

Whitney, and Wilcoxon's signed rank tests were used to assess statistical significance. Bonferroni correction was performed to adjust for the multiple comparisons. A value of $p < 0.05$ was considered statistically significant.

The Supplemental Methods section in the online-only Data Supplement provides a detailed description of the global gene expression analysis; cell culture; osteogenic differentiation; alkaline phosphatase, alizarin red (AR), and Von Kossa (VK) staining; calcium assay; reporter assays; alkaline phosphatase activity assays; fluorescence reflectance imaging *in vivo*; immunohistochemistry; immunofluorescence staining; quantitative real-time polymerase chain reaction; immunoblot assay; ELISAs; determination of DPP-4 activity; and echocardiography.

Results

DPP-4 Expression is Upregulated in the Aortic Valves of Patients with CAVD

To determine the key factors for CAVD, we investigated the global gene expression profiles involved in human CAVD using Affymetrix Gene Chip microarrays. The genes associated with calcification, fibrosis, and inflammation were upregulated in the aortic valve tissue of patients with CAVD, as compared to those of age-matched non-CAVD controls (Figure 1A). In particular, DPP-4 was significantly up-regulated in CAVD patients (Figures 1A and 1B). High DPP-4 protein expression was observed in the regions of the CAVD aortic valves with prominent calcified lesion formation, as demonstrated by AR and VK staining, and was localized in VICs, as indicated by the co-expression of DPP-4 and alpha-smooth muscle actin (α-SMA), a marker of activated myofibroblast-like VICs (Figures 1C, 1D, 1E and 1F). In contrast, the DPP-4 expression in non-CAVD human aortic valve tissue was negligible (Figure 1F).

Endothelial Nitric Oxide Deficiency Up-regulates DPP-4 Expression in Aortic Valvular Interstitial Cells

Two types of cells, VECs and VICs, in the human aortic valve contribute to normal aortic valve function.[17] To define which cell type is involved in the CAVD phenotype, we isolated the VECs and VICs from human aortic valve tissues in CAVD patients and non-CAVD controls. Only the human valvular interstitial cells (hVICs) expressing alpha-actin 2 (*ACTA2*) and cardiac beta myosin heavy chain 7 (*MYH7*) in CAVD patients exhibited a marked elevation of the osteogenic marker, alkaline phosphatase (*ALP*) mRNA (Figure 2A), which coincided with an increase in both *DPP-4* mRNA expression (Figure 2A) and the DPP-4 protein level (Figure 2B). In contrast, human valvular endothelial cells (hVECs) expressing platelet endothelial cell adhesion molecule (*PECAM1*) showed minimal differences in the *DPP-4* mRNA levels between CAVD patients and non-CAVD controls (Figure 2A). The hVECs from CAVD aortic valves expressed lower levels of endothelial nitric oxide synthase (*eNOS*) mRNA (Figure 2A) and protein (Supplementary Figure 1), as compared to those in the controls. These results suggest that prominent dysfunction in VECs and osteogenic changes in VICs are characteristic features of patients with CAVD.

Given that the administration of *Nω*-Nitro-L-arginine methyl ester, an inhibitor of nitric oxide (NO) biosynthesis, enhances DPP-4 expression in the aorta[18], we reasoned that NO depletion would trigger DPP-4 expression. NO supplemented with DETA-NONOate (DETA-NO) decreased *DPP-4* mRNA expression (Figure 2C) and DPP-4 protein expression in a dose-dependent manner in hVICs (Figure 2D). Moreover, DPP-4 protein secretion was higher in hVICs from CAVD patients than in hVICs from non-CAVD controls, and was suppressed by DETA-NO supplementation (Figure 2E).

DPP-4 Expression is Directly Regulated by NF-κB Activity, and DPP-4 Activation Results in the Osteogenic Differentiation of Aortic Valvular Interstitial Cells

NF-κB activity is known to be suppressed by NO, which is derived from endothelial cells.[19] Because the *DPP4* promoter contains a putative NF-κB binding site, we tested whether NF-κB activity directly regulates *DPP-4* promoter activity. The elevation of *DPP-4* promoter activity was reduced by DETA-NO supplementation in hVICs as well as HEK293 cells (Figure 3A and Supplementary Figure 2); however, mutating the NF-κB binding site in the *DPP-4* promoter led to a significant inhibition of *DPP-4* promoter activity, even in the absence of DETA-NO (Figure 3A). These results demonstrate that NO depletion leads to the induction of DPP-4 expression via the activation of NF-κB, suggesting a regulatory link between VECs and VICs. To obtain more direct evidence of the regulation of DPP-4 expression by NF-κB, we examined the effect of the NF-κB inhibitor on DPP-4 protein expression in hVICs. We found that the NF-κB inhibitor significantly reduced DPP-4 expression in hVICs in CAVD patients (Figure 3B).

The high levels of DPP-4 expression in hVICs from the aortic valves of CAVD cases suggest that DPP-4 plays a role in osteogenic transition, particularly in the phenotypic change from VICs to calcifying cells.[20] Thus, we examined the effects of the DPP-4 inhibitor in hVICs from CAVD patients and age-matched non-CAVD controls. Sitagliptin is a highly selective DPP-4 inhibitor that has been used for the treatment of human type 2 diabetes mellitus.[21] Sitagliptin treatment significantly attenuated the osteogenic changes in hVICs from CAVD patients *in vitro* (Figure 3C and 3D), which coincided with a decrease in the mRNA expression of osteogenic markers including *ALP*, runt-related transcription factor 2 (*RUNX2*), *Sp7* transcription factor (also known as osterix) and bone gamma-carboxyglutamic acid-containing protein (*BGLAP*; also known as osteocalcin) (Figure 3E). Moreover, we confirmed the attenuation of *in vitro*

calcification in DPP-4 knockout mouse VICs (mVICs). When compared to WT mVICs, the ALP staining and activity were significantly diminished in DPP-4 knockout mVICs, even after osteogenic stimulation (Supplementary Figure 3).

DPP-4 Induces the Osteogenic Transition of Aortic Valvular Interstitial Cells by Inactivating Insulin-Like Growth Factor-1 (IGF-1)-Mediated Signaling

We believe that the peptidase activity of DPP-4[22, 23] might promote osteogenic changes in VICs. The addition of DPP-4 and its substrate, insulin-like growth factor-1 (IGF-1), to hVICs induced osteogenic differentiation; however, none of the other DPP-4 substrates affected VIC calcification (Figure 4A). IGF-1 is known to inhibit osteogenic changes in vascular smooth muscle cells by binding to the IGF-1 receptor (IGFR) via extracellular signal-regulated protein kinase (ERK) and phosphatidylinositol 3-kinase (PI3K) activation.[24-26] The phosphorylation of ERK and Akt upon IGF-1 stimulation in hVICs was suppressed by DPP-4 (Figure 4B). A truncated form of IGF-1, resulting from DPP-4-mediated proteolytic cleavage, displays reduced binding to IGFR[23] and fails to activate the autocrine system for IGF-1 production.[27] Moreover, we found that IGF-1 production was inhibited by DPP-4, but recovered following Sitagliptin treatment (Figure 4C and 4D). DPP-4 treatment increased the osteogenic potential of hVICs in the presence of IGF-1, and this effect was abrogated by Sitagliptin treatment (Figures 4E and 4F).

The IGF-1 mRNA levels in hVICs from CAVD patients were ~2.5-fold lower than those from non-CAVD controls (Figure 4G). These findings suggest that DPP-4 limits autocrine IGF-1 signaling via the enzymatic degradation of IGF-1, thus leading to VIC calcification. Therefore, we hypothesized that IGF-1 levels could be associated with CAVD progression, and analyzed the tissue levels of IGF-1 in CAVD patients. The expression of IGF-1 protein in the aortic valve

(Figure 4H) was lower than those in non-CAVD controls, indicating a negative association between IGF-1 levels and CAVD.

Sitagliptin, a DPP-4 Inhibitor, Reduced Calcified Lesion Formation in *eNOS*$^{-/-}$ Mice by Restoring IGF-1 Signaling

Endothelial nitric oxide synthase-deficient (*eNOS*$^{-/-}$) mice are used as an animal model of aortic valve calcification.[3, 28] DPP-4 was found to be up-regulated in the calcified regions of the aortic valve leaflets of *eNOS*$^{-/-}$ mice, as demonstrated by VK-positive staining (Figure 5A). The *DPP-4* mRNA expression in the aortic valve (Figure 5B) and circulating DPP-4 protein levels (Figure 5C) were higher in *eNOS*$^{-/-}$ mice than in WT mice. Thereafter, we evaluated the efficacy of DPP-4 inhibitors for treating aortic valve calcification in *eNOS*$^{-/-}$ mice. Fluorescence reflectance imaging, with a bisphosphonate-conjugated molecular imaging agent, showed that *eNOS*$^{-/-}$ mice had much higher levels of calcification of the aortic root and valve than WT mice (Figures 5D, 5E and 5F). The oral administration of Sitagliptin decreased *in vivo* calcification (Figure 5D) as well as VK-stained regions and calcium deposition in the aortic valves of *eNOS*$^{-/-}$ mice, as compared to those receiving vehicle treatment (Figure 5E and 5F).

Moreover, Sitagliptin treatment significantly inhibited osteogenic changes in *eNOS*$^{-/-}$ mouse VICs (mVICs) *in vitro* (Figures 6A and 6B) and decreased the mRNA expression of *ALP*, *RUNX2*, *Sp7* and *BGLAP* (Figure 6C), similar to that noted in hVICs. IGF-1 treatment attenuated the osteogenic changes in *eNOS*$^{-/-}$ mVICs, which was diminished by DPP-4 treatment (Figures 6D and 6E). Sitagliptin treatment significantly inhibited DPP-4-mediated osteogenic differentiation (Figures 6D and 6E). Moreover, the plasma IGF-1 levels in *eNOS*$^{-/-}$ mice were ~3-fold lower than those in WT mice, but increased following Sitagliptin treatment (Figure 6F).

Calcific Aortic Valve Stenosis can be Prevented by DPP-4 Inhibition with Sitagliptin in a Rabbit Model of CAVD

We induced aortic valve stenosis and significant calcium deposition through a combination diet with high cholesterol and vitamin D (vit.D2) supplements in rabbits, as described previously.[29, 30] The rabbits were divided into 3 groups based on the diet and were followed for 12 weeks: 1) the control group (fed a normal diet); 2) the cholesterol-vit.D2 group, and 3) the Sitagliptin group (treated with 15 mg/kg/day of Sitagliptin, with a cholesterol-vit.D2 diet). Supplementary Table 2 summarizes the clinical and echocardiographic characteristics over the study period in all 3 groups. There was no significant difference in animal weight among the 3 groups at the time of sacrifice. The baseline echocardiographic measurements were also comparable in all 3 groups (Supplementary Table 2).

Although aortic valve cusps were thickened and became hyperechogenic after 12 weeks in the cholesterol-vit.D2 group, the administration of Sitagliptin markedly reversed cusp morphology similar to that observed in the control group (Figure 7A). Moreover, the aortic valve area (AVA), measured using the standard continuity equation, remained unchanged in the Sitagliptin group, but significantly decreased in the cholesterol-vit.D2 group (Figure 7B). Continuous-wave Doppler assessment of aortic valve function indicated that the cholesterol-vit.D2 group had much higher levels of transaortic maximal velocity at the time of 12 weeks (Figure 7C and 7D). The mean transaortic pressure gradients were also significantly increased in the cholesterol-vit.D2 group (Figure 7E). However, when Sitagliptin was orally administered, no change in the Doppler parameters was noted (Figure 7C, 7D and 7E), indicating the therapeutic effect of DPP-4 inhibition via the attenuation of cholesterol-vit.D2 diet-induced aortic valve stenosis in a rabbit model. These results support our hypothesis that the inhibition of DPP-4 can

resolve aortic valve calcification and significant aortic stenosis *in vivo*.

The therapeutic effects were observed in a dose-dependent manner, and were generally greater for rabbits receiving a higher dose (8 or 15 mg/kg) of Sitagliptin than for rabbits receiving a relatively lower dose (4 mg/kg) (Supplementary Figure 4). Despite treatment with high-dose Sitagliptin, the rabbits did not show any evidence of hypoglycemia (Supplementary Figure 5). Although the blood glucose levels were significantly higher in the cholesterol-vit.D2 group, as compared to the control group, the levels were decreased in the Sitagliptin group and remained within the normal range for rabbits at 3 weeks (Supplementary Figure 5A) and at 12 weeks (Supplementary Figure 5B)

Hematoxylin-eosin (H-E) staining demonstrated the marked thickening of the aortic valve cusps, related to increased cellularity (Masson trichrome [MT] stain), in the cholesterol-vit.D2 group, as compared to the control group (Supplementary Figure 6, Figure 8A and 8B). In contrast, the cusps from the Sitagliptin group were relatively thin, and calcium deposits (AR stain) were localized to a much lesser extent than in the cholesterol-vit.D2 group (Supplementary Figure 6, Figure 8A and 8B). A greater number of macrophages infiltrated the aortic side of the cusp in the cholesterol-vit.D2 group, whereas only a few macrophages were detected in the aortic cusps of rabbits treated with Sitagliptin (Supplementary Figure 6, Figure 8A and 8B). The plasma DPP-4 activity in the cholesterol-vit.D2 group showed a marked elevation, as compared to that in the control group at 6 and 12 weeks (Figure 8C, Supplementary Figure 7A and 8), which was associated with lower plasma IGF-1 level (Figure 8D and Supplementary Figure 7B). However, the rabbits treated with Sitagliptin displayed high plasma IGF-1 levels (Figure 8D and Supplementary Figure 7B) and significantly suppressed DPP-4 activities over a 12-week period (Figure 8C, Supplementary Figure 7A and 8). This result supports our hypothesis that low

plasma IGF-1 levels are associated with CAVD progression, and that Sitagliptin treatment significantly increased plasma IGF-1 levels, which subsequently diminished the osteogenic changes in the aortic valve leaflets and prevented CAVD progression *in vivo*.

Discussion

In the present study, we observed a novel mechanism wherein endothelial cell dysfunction, resulting in significantly low NO levels, increased the DPP-4 expression via NF-kB signaling and promoter binding in aortic VICs. Furthermore, we found that IGF-1 is a potential substrate for DPP-4 that mediates calcification, and showed that treatment with a DPP-4 inhibitor is protective against the progression of aortic valve calcification in animal models. Thus, these findings reveal potential new mechanisms of aortic valve calcification, which suggest DPP-4 and IGF-1 as mediators of osteogenic transformation in VICs.

Recently, the non-glycemic effect of DPP-4 has been reported to be beneficial in a broad spectrum of cardiovascular diseases. Genetic deletion or pharmacological inhibition of DPP-4 protects against myocardial infarction[31], ischemia/reperfusion injury[32], and cardiac hypertrophy[33] in animal models. DPP-4 inhibitors have also been found to improve endothelial dysfunction[34] and attenuate inflammation and subsequent plaque development in the vascular systems of human patients[35], thus leading to therapeutic benefits in cardiovascular disease. However, the issue of the potential association with heart failure is unclear. In a recent, large randomized study,[36] no difference was observed in the risk of hospitalization for heart failure. Moreover, a retrospective, large cohort study[37] also found no evidence of an increased risk of hospitalization for heart failure with DPP-4 inhibitors, among both patients with and without cardiovascular disease history at baseline. These reports support previous observations of the potential

beneficial effects of DPP-4 inhibition on heart failure.[38, 39] To our knowledge, this is the first report on the non-glycemic function of DPP-4 as part of the mechanism of valvular heart disease, particularly in aortic valve calcification. We suggest that the main mechanisms of CAVD development and progression are the DPP-4 overexpression which is triggered by endothelial dysfunction, and the increased enzymatic activity which leads to the suppression of IGF-1 activity.

IGF-1 is an anabolic growth hormone with pleiotropic actions on the cardiovascular system.[40] IGF-1 signaling regulates contractility, metabolism, hypertrophy, autophagy, senescence, and apoptosis in the heart. IGF-1 deficiency is associated with an increased risk of cardiovascular disease, whereas the cardiac activation of the IGF-1 receptor protects against the detrimental effects of a high fat diet and myocardial infarction.[41] Moreover, IGF-1 was found to protect against endothelial dysfunction, atherosclerotic plaque development, and metabolic syndrome, thus indicating that IGF-1 can serve as a vascular protective factor.[42] The protective effect of IGF1 on the proliferation and osteoblastic differentiation of calcifying vascular smooth muscle cells has already been reported.[43,44] Along with the coincidental vascular calcification with bone loss or osteoporosis, regulatory mechanisms of IGF1 on vascular smooth muscle cell phenotypic transformation to osteogenic-like cells were considered to have potential clinical implication for osteoporosis therapy.[44] However, its potential implication for regulation of osteogenic differentiation of VICs has yet to be reported. In the present study, we sought to identify the other important roles of IGF-1 signaling in the onset and progression of CAVD. In particular, we determined the critical role of IGF-1 signaling in the downstream mechanism after DPP-4 activation in CAVD through mechanistic studies on cultured human VICs. The addition of DPP-4 and IGF-1, as its substrate, to human VICs induced osteogenic differentiation; however,

none of the other DPP-4 substrates affected VIC calcification. We found that IGF-1 production was inhibited by DPP-4, which recovered following the administration of a specific DPP-4 inhibitor, Sitagliptin. Furthermore, the administration of the DPP-4 inhibitor reduced the osteogenic changes in hVICs and mVICs by re-establishing the activity of IGF-1 (Supplementary Figure 9) and direct inhibition of IGF1 signaling using IGF-1 receptor antagonist resulted in enhancement of in vitro calcification of hVICs and increased aortic valve calcification in eNOS$^{-/-}$ mice (Supplementary Figure 10). These observations suggest direct relationship between DPP-4 and IGF-1, thereby adding support to the notion that DPP-4 and IGF-1 are key proteins regulating valvular calcification. Considering the current lack of medical therapy for CAVD, these findings have potential clinical implications suggesting a novel target of CAVD with a new molecular mechanism. As IGF-1 also protects against fibrosis[41,45] an earlier pathologic process in CAVD progression[46], targeting the IGF-1 pathway to protect both fibrosis and calcification provides a theoretical advantage to prevent CAVD development and progression, as compared to targeting other pathways that affect calcification alone.[47, 48]

The most interesting finding in the present study is a regulatory link between VECs and VICs that plays a critical role in the osteogenic transformation of VICs and CAVD progression (Supplementary Figure 8). The functional relationship between VECs and VICs in the aortic valve is intrinsic to the maintenance of aortic valve tissue homeostasis and the prevention of calcification.[49, 50] In the present study, we found that NO depletion in human VECs leads to the induction of DPP-4 expression via NF-kB activation in human VICs. Moreover, we noted that the alteration of DPP4 activity induces the suppression of IGF-1 signaling, which leads to the transdifferentiation of VICs to osteogenic cells. These results suggest that the interaction between VECs and VICs is important in regulating DPP-4 activity and IGF-1 signaling as novel

mediators of osteogenic transformation of VICs (Supplementary Figure 11). Our findings support the hypothesis that endothelial dysfunction contributes to CAVD by initiating the calcification of the neighboring VICs in a paracrine manner.[51]

In summary, we found that DPP-4 was a potential player in aortic valve calcification, and showed that DPP-4 could serve as a novel molecular therapeutic target for treating CAVD. Given that there is no effective treatment option other than invasive valve replacement procedures in patients with advanced CAVD, successful repositioning of DPP-4 inhibitors to halt CAVD progression is expected to result in a revolutionary paradigm shift in the management of patients with CAVD.

Limitations

We assessed the levels of DPP-4 or IGF-1 in cultured VICs from patients with CAVD and also in animal models of aortic valve calcification. However, in the present study, it was not possible to fully evaluate whether the plasma levels of DPP-4 and IGF-1 were useful biomarkers for CAVD. In particular, such a finding cannot be made through a single observation in a small cohort of aortic stenosis patients. Thus, further proof-of-concept studies and applications in a large population are needed to obtain sufficient evidence to support the potential use of DPP-4 and IGF-1 as biomarkers in CAVD. However, the absence of these supporting data would not diminish the importance of the DPP-4–IGF-1 axis in the pathogenesis of CAVD, as we believe that the local alterations of DPP-4 activity and IGF-1 signaling in aortic valve tissue, rather than the systemic changes in the plasma, would be more important in the pathophysiological processes leading to CAVD in humans.

Although our *in vivo* observations in mice and rabbits were consistent with *in vitro* data using VICs from CAVD patients, the clinical efficacy of DPP-4 inhibitors needs to be further

tested. There may be some differences in the distribution of various DPP-4 inhibitors in organs and tissues. Hence, it is crucial to define an adequate dose of a specific DPP-4 inhibitor, in compliance with its tissue distribution, that is most effective for attenuating the non-glycemic function of DPP-4 to halt CAVD progression. Furthermore, the potential impact of our novel pathway on other possible calcification mechanisms, including circulating progenitors[52], endothelial-to-mesenchymal transition[53], and non-osteogenic calcification,[54] needs to be evaluated.

Thus, our results show that DPP-4-dependent IGF-1 inhibition in VICs contributes to the osteogenic differentiation of valve cells, and leads to aortic valve calcification. We believe that this may be a novel mechanism underlying CAVD, and suggest that DPP-4 could serve as a potential therapeutic target to halt CAVD progression.

Acknowledgements

The authors are grateful to Sung-Cheol Yun, PhD for providing the statistical support.

Sources of Funding

This work was supported by grants of the Korea Health Technology R&D Project, funded by the Ministry of Health & Welfare, Republic of Korea (A100591, HI14C19160000 and HI16C0225), and the Basic Science Research Program funded by the Ministry of Education, Science, and Technology (2013R1A1A3010455). The project was also supported by grants of the National Research Foundation of Korea funded by the Ministry of Education (2014R1A6A3A04056205), the Korean Government, MSIP (2008-0062286 and 2016M3A9E8941332) and by a grant (14-021) from the Asan Institute for Life Sciences and Corporate Relations of the Asan Medical

Center, Seoul, Korea.

Disclosures

The authors declare no competing financial interests.

References

1. Rajamannan NM, Evans FJ, Aikawa E, Grande-Allen KJ, Demer LL, Heistad DD, Simmons CA, Masters KS, Mathieu P, O'Brien KD, Schoen FJ, Towler DA, Yoganathan AP and Otto CM. Calcific aortic valve disease: not simply a degenerative process: A review and agenda for research from the National Heart and Lung and Blood Institute Aortic Stenosis Working Group. Executive summary: Calcific aortic valve disease-2011 update. *Circulation*. 2011;124:1783-1791.
2. Freeman RV and Otto CM. Spectrum of calcific aortic valve disease: pathogenesis, disease progression, and treatment strategies. *Circulation*. 2005;111:3316-3326.
3. Sider KL, Blaser MC and Simmons CA. Animal models of calcific aortic valve disease. *Int J Inflam*. 2011;2011:364310. doi: 10.4061/2011/364310.
4. Dweck MR, Boon NA and Newby DE. Calcific aortic stenosis: a disease of the valve and the myocardium. *J Am Coll Cardiol*. 2012;60:1854-1863. doi: 10.1016/j.jacc.2012.02.093.
5. Aikawa E, Nahrendorf M, Sosnovik D, Lok VM, Jaffer FA, Aikawa M and Weissleder R. Multimodality molecular imaging identifies proteolytic and osteogenic activities in early aortic valve disease. *Circulation*. 2007;115:377-386.
6. Yutzey KE, Demer LL, Body SC, Huggins GS, Towler DA, Giachelli CM, Hofmann-Bowman MA, Mortlock DP, Rogers MB, Sadeghi MM and Aikawa E. Calcific aortic valve disease: a consensus summary from the Alliance of Investigators on Calcific Aortic Valve Disease. *Arterioscler Thromb Vasc Biol*. 2014;34:2387-2393. doi: 10.1161/ATVBAHA.114.302523.
7. Dweck MR, Khaw HJ, Sng GK, Luo EL, Baird A, Williams MC, Makiello P, Mirsadraee S, Joshi NV, van Beek EJ, Boon NA, Rudd JH and Newby DE. Aortic stenosis, atherosclerosis, and skeletal bone: is there a common link with calcification and inflammation? *Eur Heart J*. 2013;34:1567-1574. doi: 10.1093/eurheartj/eht034.
8. Rossebo AB, Pedersen TR, Boman K, Brudi P, Chambers JB, Egstrup K, Gerdts E, Gohlke-Barwolf C, Holme I, Kesaniemi YA, Malbecq W, Nienaber CA, Ray S, Skjaerpe T, Wachtell K and Willenheimer R. Intensive lipid lowering with simvastatin and ezetimibe in aortic stenosis. *N Engl J Med*. 2008;359:1343-1356. doi: 10.1056/NEJMoa0804602.
9. Chan KL, Teo K, Dumesnil JG, Ni A and Tam J. Effect of Lipid lowering with rosuvastatin on progression of aortic stenosis: results of the aortic stenosis progression observation: measuring effects of rosuvastatin (ASTRONOMER) trial. *Circulation*. 2010;121:306-314. doi: 10.1161/CIRCULATIONAHA.109.900027.
10. Rajamannan NM, Subramaniam M, Rickard D, Stock SR, Donovan J, Springett M, Orszulak T, Fullerton DA, Tajik AJ, Bonow RO and Spelsberg T. Human aortic valve

calcification is associated with an osteoblast phenotype. *Circulation*. 2003;107:2181-2184.
11. Hjortnaes J, Shapero K, Goettsch C, Hutcheson JD, Keegan J, Kluin J, Mayer JE, Bischoff J and Aikawa E. Valvular interstitial cells suppress calcification of valvular endothelial cells. *Atherosclerosis*. 2015;242:251-260. doi: 10.1016/j.atherosclerosis.2015.07.008.
12. Otto CM and Prendergast B. Aortic-valve stenosis--from patients at risk to severe valve obstruction. *N Engl J Med*. 2014;371:744-756. doi: 10.1056/NEJMra1313875.
13. Zaruba MM, Theiss HD, Vallaster M, Mehl U, Brunner S, David R, Fischer R, Krieg L, Hirsch E, Huber B, Nathan P, Israel L, Imhof A, Herbach N, Assmann G, Wanke R, Mueller-Hoecker J, Steinbeck G and Franz WM. Synergy between CD26/DPP-IV inhibition and G-CSF improves cardiac function after acute myocardial infarction. *Cell stem cell*. 2009;4:313-323. doi: 10.1016/j.stem.2009.02.013.
14. Ohnuma K, Dang NH and Morimoto C. Revisiting an old acquaintance: CD26 and its molecular mechanisms in T cell function. *Trends Immunol*. 2008;29:295-301. doi: 10.1016/j.it.2008.02.010.
15. Stonehouse AH, Darsow T and Maggs DG. Incretin-based therapies. *J Diabetes*. 2012;4:55-67. doi: 10.1111/j.1753-0407.2011.00143.x.
16. Pratley RE and Salsali A. Inhibition of DPP-4: a new therapeutic approach for the treatment of type 2 diabetes. *Curr Med Res Opin*. 2007;23:919-931.
17. Leopold JA. Cellular mechanisms of aortic valve calcification. *Circ Cardiovasc Interv*. 2012;5:605-614. doi: 10.1161/CIRCINTERVENTIONS.112.971028.
18. Linardi A, Panunto PC, Ferro ES and Hyslop S. Peptidase activities in rats treated chronically with N(omega)-nitro-L-arginine methyl ester (L-NAME). *Biochem Pharmacol*. 2004;68:205-214.
19. Colasanti M and Persichini T. Nitric oxide: an inhibitor of NF-kappaB/Rel system in glial cells. *Brain Res Bull*. 2000;52:155-161.
20. Chen JH, Yip CY, Sone ED and Simmons CA. Identification and characterization of aortic valve mesenchymal progenitor cells with robust osteogenic calcification potential. *Am J Pathol*. 2009;174:1109-1119. doi: 10.2353/ajpath.2009.080750.
21. Moller DE. Metabolic disease drug discovery- "hitting the target" is easier said than done. *Cell metab*. 2012;15:19-24. doi: 10.1016/j.cmet.2011.10.012.
22. Muskiet MH, Smits MM, Morsink LM and Diamant M. The gut-renal axis: do incretin-based agents confer renoprotection in diabetes? *Nat Rev Nephrol*. 2014;10:88-103. doi: 10.1038/nrneph.2013.272.
23. Lin CT, Tang HY, Han YS, Liu HP, Huang SF, Chien CH, Shyy J, Chiu JJ and Chen X. Downregulation of Signaling-active IGF-1 by Dipeptidyl Peptidase IV (DPP-IV). *Int J Biomed Sci*. 2010;6:301-309.
24. Radcliff K, Tang TB, Lim J, Zhang Z, Abedin M, Demer LL and Tintut Y. Insulin-like growth factor-I regulates proliferation and osteoblastic differentiation of calcifying vascular cells via extracellular signal-regulated protein kinase and phosphatidylinositol 3-kinase pathways. *Circ Res*. 2005;96:398-400.
25. Siddals KW, Allen J, Sinha S, Canfield AE, Kalra PA and Gibson JM. Apposite insulin-like growth factor (IGF) receptor glycosylation is critical to the maintenance of vascular smooth muscle phenotype in the presence of factors promoting osteogenic differentiation and mineralization. *J Biol Chem*. 2011;286:16623-16630. doi: 10.1074/jbc.M110.202929.
26. Loddick SA, Liu XJ, Lu ZX, Liu C, Behan DP, Chalmers DC, Foster AC, Vale WW, Ling N and De Souza EB. Displacement of insulin-like growth factors from their binding

proteins as a potential treatment for stroke. *Proc Natl Acad Sci U S A*. 1998;95:1894-1898.
27. Clemmons DR. Modifying IGF1 activity: an approach to treat endocrine disorders, atherosclerosis and cancer. *Nat Rev Drug Discov*. 2007;6:821-833.
28. El Accaoui RN, Gould ST, Hajj GP, Chu Y, Davis MK, Kraft DC, Lund DD, Brooks RM, Doshi H, Zimmerman KA, Kutschke W, Anseth KS, Heistad DD and Weiss RM. Aortic valve sclerosis in mice deficient in endothelial nitric oxide synthase. *Am J Physiol Heart Circ Physiol*. 2014;306:H1302-1313. doi: 10.1152/ajpheart.00392.2013.
29. Drolet MC, Couet J and Arsenault M. Development of aortic valve sclerosis or stenosis in rabbits: role of cholesterol and calcium. *J Heart Valve Dis*. 2008;17:381-387.
30. Drolet MC, Arsenault M and Couet J. Experimental aortic valve stenosis in rabbits. *J Am Coll Cardiol*. 2003;41:1211-1217.
31. Sauve M, Ban K, Momen MA, Zhou YQ, Henkelman RM, Husain M and Drucker DJ. Genetic deletion or pharmacological inhibition of dipeptidyl peptidase-4 improves cardiovascular outcomes after myocardial infarction in mice. *Diabetes*. 2010;59:1063-1073. doi: 10.2337/db09-0955.
32. Ku HC, Chen WP and Su MJ. DPP4 deficiency preserves cardiac function via GLP-1 signaling in rats subjected to myocardial ischemia/reperfusion. *Naunyn Schmiedebergs Arch Pharmacol*. 2011;384:197-207. doi: 10.1007/s00210-011-0665-3.
33. Miyoshi T, Nakamura K, Yoshida M, Miura D, Oe H, Akagi S, Sugiyama H, Akazawa K, Yonezawa T, Wada J and Ito H. Effect of vildagliptin, a dipeptidyl peptidase 4 inhibitor, on cardiac hypertrophy induced by chronic beta-adrenergic stimulation in rats. *Cardiovasc Diabetol*. 2014;13:43. doi: 10.1186/1475-2840-13-43.
34. Rizzo M, Rizvi AA, Spinas GA, Rini GB and Berneis K. Glucose lowering and anti-atherogenic effects of incretin-based therapies: GLP-1 analogues and DPP-4-inhibitors. *Expert Opin Investig Drugs*. 2009;18:1495-1503. doi: 10.1517/14728220903241633.
35. Zhong J, Rao X and Rajagopalan S. An emerging role of dipeptidyl peptidase 4 (DPP4) beyond glucose control: potential implications in cardiovascular disease. *Atherosclerosis*. 2013;226:305-314. doi: 10.1016/j.atherosclerosis.2012.09.012.
36. Green JB, Bethel MA, Armstrong PW, Buse JB, Engel SS, Garg J, Josse R, Kaufman KD, Koglin J, Korn S, Lachin JM, McGuire DK, Pencina MJ, Standl E, Stein PP, Suryawanshi S, Van de Werf F, Peterson ED, Holman RR and Group TS. Effect of Sitagliptin on Cardiovascular Outcomes in Type 2 Diabetes. *N Engl J Med*. 2015;373:232-242. doi: 10.1056/NEJMoa1501352.
37. Fu AZ, Johnston SS, Ghannam A, Tsai K, Cappell K, Fowler R, Riehle E, Cole AL, Kalsekar I and Sheehan J. Association Between Hospitalization for Heart Failure and Dipeptidyl Peptidase 4 Inhibitors in Patients With Type 2 Diabetes: An Observational Study. *Diabetes Care*. 2016;39:726-734. doi: 10.2337/dc15-0764.
38. Shigeta T, Aoyama M, Bando YK, Monji A, Mitsui T, Takatsu M, Cheng XW, Okumura T, Hirashiki A, Nagata K and Murohara T. Dipeptidyl peptidase-4 modulates left ventricular dysfunction in chronic heart failure via angiogenesis-dependent and -independent actions. *Circulation*. 2012;126:1838-1851. doi: 10.1161/CIRCULATIONAHA.112.096479.
39. dos Santos L, Salles TA, Arruda-Junior DF, Campos LC, Pereira AC, Barreto AL, Antonio EL, Mansur AJ, Tucci PJ, Krieger JE and Girardi AC. Circulating dipeptidyl peptidase IV activity correlates with cardiac dysfunction in human and experimental heart failure. *Circ Heart Fail*. 2013;6:1029-1038. doi: 10.1161/CIRCHEARTFAILURE.112.000057.
40. Troncoso R, Ibarra C, Vicencio JM, Jaimovich E and Lavandero S. New insights into

IGF-1 signaling in the heart. *Trends Endocrinol Metab*. 2014;25:128-137. doi: 10.1016/j.tem.2013.12.002.
41. Li Q, Li B, Wang X, Leri A, Jana KP, Liu Y, Kajstura J, Baserga R and Anversa P. Overexpression of insulin-like growth factor-1 in mice protects from myocyte death after infarction, attenuating ventricular dilation, wall stress, and cardiac hypertrophy. *J Clin Invest*. 1997;100:1991-1999.
42. Conti E, Carrozza C, Capoluongo E, Volpe M, Crea F, Zuppi C and Andreotti F. Insulin-like growth factor-1 as a vascular protective factor. *Circulation*. 2004;110:2260-2265.
43. Radiff K, Tang TB, Lim J, Zhang Z, Abedin M, Demer LL, Tintut Y. Insulin-like growth factor-1 regulates proliferation and osteoblastic differentiation of calcifying vascular cells via extracellular signal-regulated protein kinase and phosphatidylinositol 3-kinase pathways. *Circ Res.* 2005;96:398-400.
44. di Bartolo BA, Schoppet M, Mattar MZ, Rachner TD, Shanahan CM, Kavurma MM. Calcium and osteoprotegerin regulate IGF1R expression to inhibit vascular calcification. *Cardiovasc Res.* 2011;91:537-545. doi: 10.1093/cvr/cvr084.
45. Huynh K, McMullen JR, Julius TL, Tan JW, Love JE, Cemerlang N, Kiriazis H, Du XJ and Ritchie RH. Cardiac-specific IGF-1 receptor transgenic expression protects against cardiac fibrosis and diastolic dysfunction in a mouse model of diabetic cardiomyopathy. *Diabetes*. 2010;59:1512-1520. doi: 10.2337/db09-1456.
46. Weiss RM, Miller JD and Heistad DD. Fibrocalcific aortic valve disease: opportunity to understand disease mechanisms using mouse models. *Circ Res*. 2013;113:209-222. doi: 10.1161/CIRCRESAHA.113.300153.
47. Mahmut A, Boulanger MC, El Husseini D, Fournier D, Bouchareb R, Despres JP, Pibarot P, Bosse Y and Mathieu P. Elevated expression of lipoprotein-associated phospholipase A2 in calcific aortic valve disease: implications for valve mineralization. *J Am Coll Cardiol*. 2014;63:460-469. doi: 10.1016/j.jacc.2013.05.105.
48. Kamstrup PR, Tybjaerg-Hansen A and Nordestgaard BG. Elevated lipoprotein(a) and risk of aortic valve stenosis in the general population. *J Am Coll Cardiol*. 2014;63:470-477. doi: 10.1016/j.jacc.2013.09.038.
49. Liu AC, Joag VR and Gotlieb AI. The emerging role of valve interstitial cell phenotypes in regulating heart valve pathobiology. *Am J Pathol*. 2007;171:1407-1418.
50. Richards J, El-Hamamsy I, Chen S, Sarang Z, Sarathchandra P, Yacoub MH, Chester AH and Butcher JT. Side-specific endothelial-dependent regulation of aortic valve calcification: interplay of hemodynamics and nitric oxide signaling. *Am J Pathol*. 2013;182:1922-1931. doi: 10.1016/j.ajpath.2013.01.037.
51. Bosse K, Hans CP, Zhao N, Koenig SN, Huang N, Guggilam A, LaHaye S, Tao G, Lucchesi PA, Lincoln J, Lilly B and Garg V. Endothelial nitric oxide signaling regulates Notch1 in aortic valve disease. *J Mol Cell Cardiol*. 2013;60:27-35. doi: 10.1016/j.yjmcc.2013.04.001.
52. Gossl M, Khosla S, Zhang X, Higano N, Jordan KL, Loeffler D, Enriquez-Sarano M, Lennon RJ, McGregor U, Lerman LO and Lerman A. Role of circulating osteogenic progenitor cells in calcific aortic stenosis. *J Am Coll Cardiol*. 2012;60:1945-1953. doi: 10.1016/j.jacc.2012.07.042.
53. Paranya G, Vineberg S, Dvorin E, Kaushal S, Roth SJ, Rabkin E, Schoen FJ and Bischoff J. Aortic valve endothelial cells undergo transforming growth factor-beta-mediated and non-transforming growth factor-beta-mediated transdifferentiation in vitro. *Am J Pathol*. 2001;159:1335-1343.

54. Chu Y, Lund DD, Weiss RM, Brooks RM, Doshi H, Hajj GP, Sigmund CD and Heistad DD. Pioglitazone attenuates valvular calcification induced by hypercholesterolemia. *Arterioscler Thromb Vasc Biol*. 2013;33:523-532. doi: 10.1161/ATVBAHA.112.300794.

Figure Legends

Figure 1. Upregulation of Dipeptidyl Peptidase-4 (DPP-4) Expression in Human Aortic Valve Tissue from a Calcific Aortic Valve Disease (CAVD) Patient

(A) Gene expression profiles of calcification, fibrosis, and inflammation in aortic valve tissue. Upregulated and downregulated transcripts are shown in red and green, respectively. The columns correspond to aortic valve samples without (non-CAVD #1–3) and with (CAVD #1–3) CAVD. The heat map is scaled at the row level to compare expression profiles between samples for a given probe set.

(B) mRNA level of human *DPP-4* (h*DPP-4*) was validated by performing qRT-PCR in aortic valves from non-CAVD (*n*=8) and CAVD samples (*n*=10). The expression values of the samples are shown relative to that of the *GAPDH* reference gene. Values represent fold changes of the mean value measured in the non-CAVD controls.

(C) Aortic valves from non-CAVD and CAVD patients were stained with alizarin red (AR), Von Kossa (VK), 4′,6-diamidino-2-phenylindole (DAPI), hDPP-4, and alpha-smooth muscle actin (α-SMA) staining. Merged images (DAPI, hDPP-4, and α-SMA) are shown. Nuclei were stained with DAPI (blue). Scale bar, 100 μm. (D) The bar graph presents the AR-positive area and (E) VK-positive area measured in each aortic valve from non-CAVD (*n*=8) and CAVD samples (*n*=10). (F) The DPP-4 expression level in the aortic valve is represented as a percentage of immunoreactive cells in the aortic valves of non-CAVD (*n*=8) and CAVD samples (*n*=10). Error bars represent the standard deviation. *p* values were obtained using Student's *t* tests.

Figure 2. Induction of DPP-4 Expression in Aortic Valve Cells via Nitric Oxide Deprivation

(A) qRT-PCR analysis of *PECAM1*, *ACTA2 (α-SMA)*, *MYH7*, *ALP*, *DPP-4*, and *eNOS* from hVECs and hVICs in non-CAVD controls (n=8) and CAVD patients (n=10). Values represent fold changes of the mean value measured in the non-CAVD hVEC group.

(B) The levels of hDPP-4 protein in conditioned media (CM) were measured in hVECs and hVICs of non-CAVD and CAVD patients, using ELISA.

(C) h*DPP-4* mRNA levels in hVICs treated with DETA-NO, as determined by qRT-PCR. Values represent the fold changes of the mean value measured in the vehicle.

(D) Immunoblot analysis of hDPP-4 and β-actin from hVICs treated with DETA-NO for 48 h. Quantification of the hDPP-4 density relative to β-actin. Values represent fold changes of the mean value measured for vehicle treatment.

(E) hDPP-4 protein levels in CM from non-CAVD and CAVD patients. hVICs treated with DETA-NO were assessed using ELISA. Data represent the mean±standard deviation. *p* values were obtained using Student's *t* tests.

Figure 3. DPP-4 Upregulation via Nitric Oxide Deprivation-Dependent NF-κB Activation Results in Osteogenic Transdifferentiation of Aortic Valve Interstitial Cells

(A) Schematic of the putative NF-κB binding site in the DPP-4 promoter. The underlined letters indicate mutations (MT) in the NF-κB binding site. h*DPP-4* promoter activity was measured in VICs after transfection with either the luciferase constructs of the wild-type (WT) or MT h*DPP-4* promoters followed by treatment with DETA-NO.

(B) hDPP-4 levels in CM from non-CAVD and CAVD patients. hVICs treated with an NF-κB transcriptional activation inhibitor were measured using ELISA.

(C) AR staining of non-CAVD and CAVD patient hVICs in the presence or absence of Sitagliptin (100 μM) after 4 weeks of osteogenic stimulation. The bar graph presents the AR-positive area measured in each culture dish.

(D) The calcium concentration in the cells from Figure 3C was measured, as described in the Supplemental Methods section in the online-only Data Supplement.

(E) qRT-PCR analysis of *ALP*, *RUNX2*, *Sp7* and *BGLAP* mRNA from hVICs of non-CAVD and CAVD patients, followed by treatment with Sitagliptin. Data represent the mean±standard deviation. *p* values were obtained using Student's *t* tests.

Figure 4. DPP-4 Inactivates IGF-1-Mediated Signaling to Induce Osteogenesis in Human Valvular Interstitial Cells (hVICs) *in vitro*

(A) Alkaline phosphatase (ALP) activity was determined in hVICS of non-CAVD and CAVD patients after treatment with substrates alone or with substrates pretreated with DPP-4 after 1 week of osteogenic stimulation. White bars: vehicle, Black bars: DPP-4 treatment. Mock, Endomorphin-2, gastrin-releasing peptide (GRP), peptide histidine methionine 27 (PHM27), glucagon-like peptide-2 (GLP-2), peptide YY, chromogranin A, Substance P, aprotinin, bradykinin, neuropeptide-Y (NPY), glucagon-like peptide-1 (GLP-1), or insulin-like growth factor-1 (IGF-1) (concentration of all substrates was 200 ng/ml) in the presence or absence of DPP-4 (50 ng/ml).

(B) Immunoblot analysis of pERK, ERK, pAkt, Akt, and β-actin expression in hVICs treated with IGF-1 (50 ng/ml) or IGF-1+DPP-4 (50 ng/ml each) at the indicated times. Quantification of the pERK, ERK, pAkt, and Akt densities relative to β-actin. Values represent the fold changes of the mean value measured at 0 min.

(C) h*IGF-1* mRNA expression, as determined by qRT-PCR, in the hVICs after 24 h treatment with IGF-1 (50 ng/ml) alone or with IGF-1+DPP-4 (50 ng/ml each) in the presence or absence of Sitagliptin (100 μM). Values represent the fold changes of the mean value measured in the controls.

(D) hIGF-1 protein levels in CM from hVICs treated with DPP-4 (50 ng/ml) in the presence or absence of Sitagliptin.

(E) Alizarin red (AR)-positive areas were determined after 4 weeks of osteogenic stimulation (OM) in the hVICs treated as in (C). Values represent the percentage of AR-positive areas compared to the control.

(F) The calcium concentration in the cells from Figure 4D was determined.

(G) qRT-PCR analysis of *IGF-1* from hVECs and hVICs of non-CAVD and CAVD patients. Values represent the fold changes of the mean value measured in the non-CAVD hVEC. Data represent the mean±standard deviation. *p* values were obtained using Student's *t* tests.

(H) Immunofluorescence staining of IGF-1 in the aortic valves of non-CAVD and CAVD patients. Nuclei were stained with DAPI (blue). Merged images (DAPI and IGF-1) are shown. Scale bar, 100 μm.

Figure 5. Attenuation of *in vivo* Calcification by DPP-4 Inhibition

(A) Paraffin-embedded cross sections of the aortic valve from WT and *eNOS*$^{-/-}$ mice stained with Von Kossa (VK) and antibodies against murine DPP-4 (mDPP-4). H-E, hematoxylin and eosin; MT, Masson's trichrome stain. The arrows indicate the calcified lesions. The arrowheads indicate the mDPP-4-positive area. Scale bar, 100 μm.

(B) m*DPP-4* mRNA expression in the aortic valve, as determined by qRT-PCR. Values represent

the fold changes of the mean value measured in the controls (*n*=7 per group).

(C) Comparison of the plasma levels of mDPP-4 in WT and *eNOS*$^{-/-}$ mice, as determined using ELISA (*n*=7 per group).

(D) WT and *eNOS*$^{-/-}$ mice were administered with vehicle or Sitagliptin (15 mg/kg/day) orally for 12 weeks. Molecular imaging of aortic valve calcification *in vivo* after the injection of a fluorescent agent (Osteosense680) and quantification of fluorescence in WT and *eNOS*$^{-/-}$ mice (*n*=7 per group). Values represent the fold changes of the mean value measured in vehicle treatment.

(E) Aortic valve cusp sections were stained with VK to detect prominent calcified lesions. The arrows indicate the calcified lesions. Scale bar, 100 μm. Quantification of the VK-positive areas (% of the aortic valve). Values represent the percentage of VK-positive areas compared to the vehicle treatment.

(F) Calcium content in the aortic valve cusp was measured (*n*=7 per group). Data represent the mean±standard deviation. *p* values were obtained using Student's *t* tests.

Figure 6. Attenuation of *in vitro* Calcification is Associated with an Increase in the IGF-1 Level by DPP-4 Inhibition

(A) Alizarin red (AR) staining of WT and *eNOS*$^{-/-}$ mVICs in the presence or absence of Sitagliptin (100 μM) after 4 weeks of osteogenic stimulation (OM). The bar graph presents the AR-positive area measured in each culture dish.

(B) The calcium concentration in the cells from Figure 6A was determined.

(C) qRT-PCR analysis of *ALP*, *RUNX2*, *Sp7* and *BGLAP* from mVICs of WT and *eNOS*$^{-/-}$ mice, followed by treatment with Sitagliptin.

(D) AR-positive areas were determined after 4 weeks of OM in *eNOS*$^{-/-}$ mVICs treated with IGF-1 (50 ng/ml) alone, or IGF-1+DPP-4 (50 ng/ml each) in the presence or absence of Sitagliptin (100 μM). Values represent the percentage of AR-positive areas compared to the control.

(E) The calcium content in the cells from Figure 6D was measured.

(F) The levels of mIGF-1 in plasma were measured in WT and *eNOS*$^{-/-}$ mice treated with vehicle or Sitagliptin (n=7 per group). Data represent the mean±standard deviation. p values were obtained using Student's t tests.

Figure 7. Effect of Sitagliptin on the Aortic Valve in a CAVD rabbit model, as Determined by Echocardiographic Assessment

(A) Representative two-dimensional echocardiographic images of the aortic valve cusp at 12 weeks after treatment initiation. The aortic valves were imaged in the parasternal short axis (upper panels) and long axis (lower panels) views to assess valve morphology. In the control group fed a normal diet, the aortic valve shows a thin structure that was barely visible. However, in rabbits fed with high cholesterol and vitamin D2 supplements (Chol+Vit.D2), the aortic cusps had become thickened and hyperechogenic (arrows). Treatment with Sitagliptin (Chol+Vit.D2 +Sitagliptin) could reverse the valve morphology to a similar state as in the control group.

(B) The aortic valve area (AVA) was measured using the standard continuity equation.

(C) Continuous-wave Doppler was used to measure the integral of the transvalvular flow to be utilized in the continuity equation for AVA calculation, and to record the trans-aortic (D) peak velocity (Vmax), and (E) mean pressure gradients. Data represent the mean±standard deviation. p values were obtained using nonparametric matched data analysis; Wilcoxon's signed rank test.

Figure 8. Immunohistochemical Staining of Rabbit Aortic Valve Cusps, with Measurements of the Plasma DPP-4 Activity and IGF-1 Level

(A) Light microscopy of the cross-sectional tissue of rabbit aortic valve with immuno-histochemical staining (Scale bar, 100 μm). A low-magnification view of these images was provided in Figure S5. (B) Longitudinal section of rabbit aortic cusps attached to the aortic root. An asterisk indicates the aortic side of the cusp (Scale bar, 200 μm). Hematoxylin-eosin (H-E) staining demonstrates marked thickening on the aortic side of the cusp in the Chol+Vit.D2 group. This thickening is associated with an increase in cellularity (Masson trichrome stain: MT), macrophage infiltration (RAM-11 immunostain), and calcification (alizarin red stain: AR). (C) Plasma DPP-4 activity and (D) IGF-1 levels were measured at baseline and at 3, 6, or 12 weeks. There were at least 5 animals in each group. Data represent the mean±standard deviation. *p* values were obtained using nonparametric Mann-Whitney test.

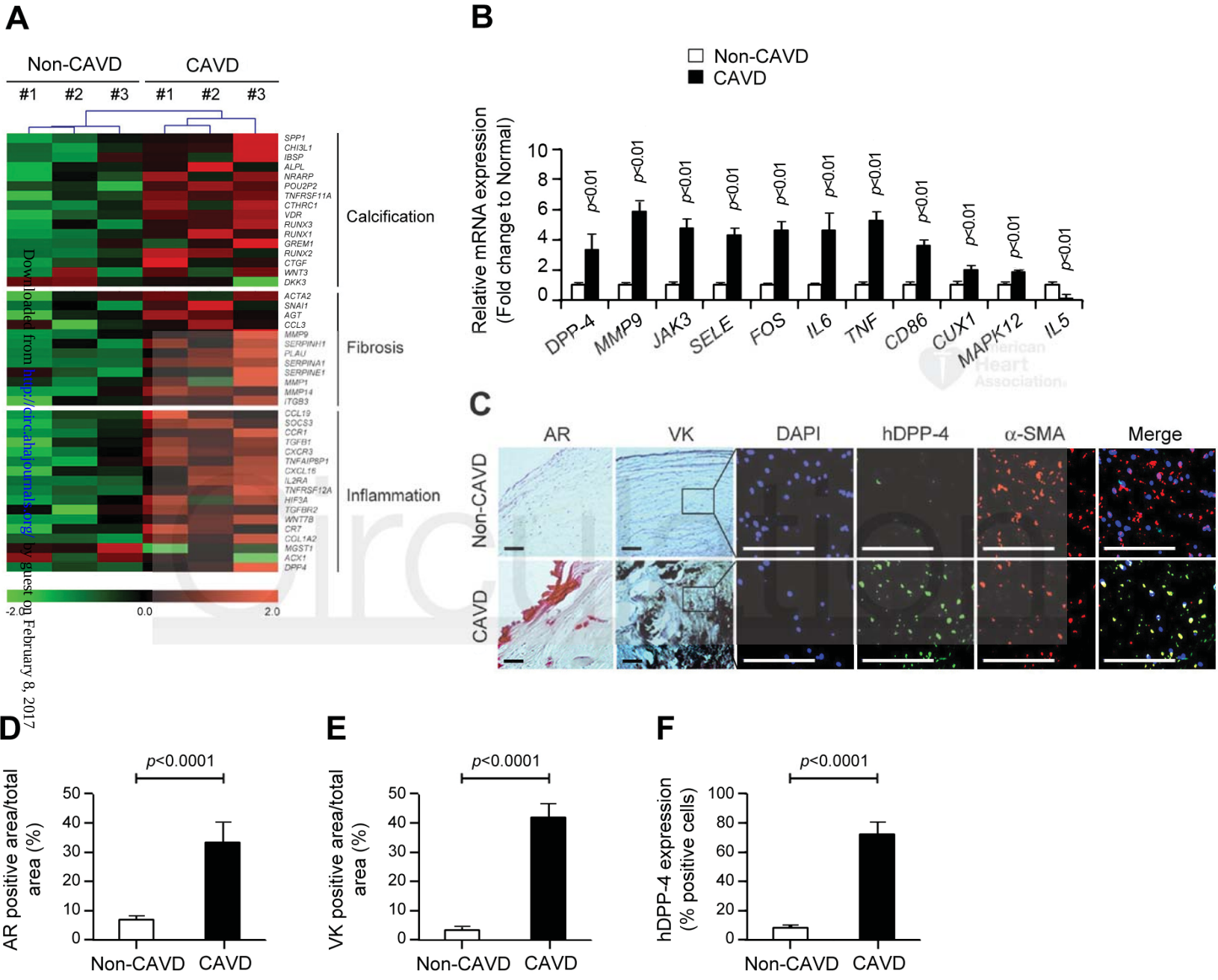

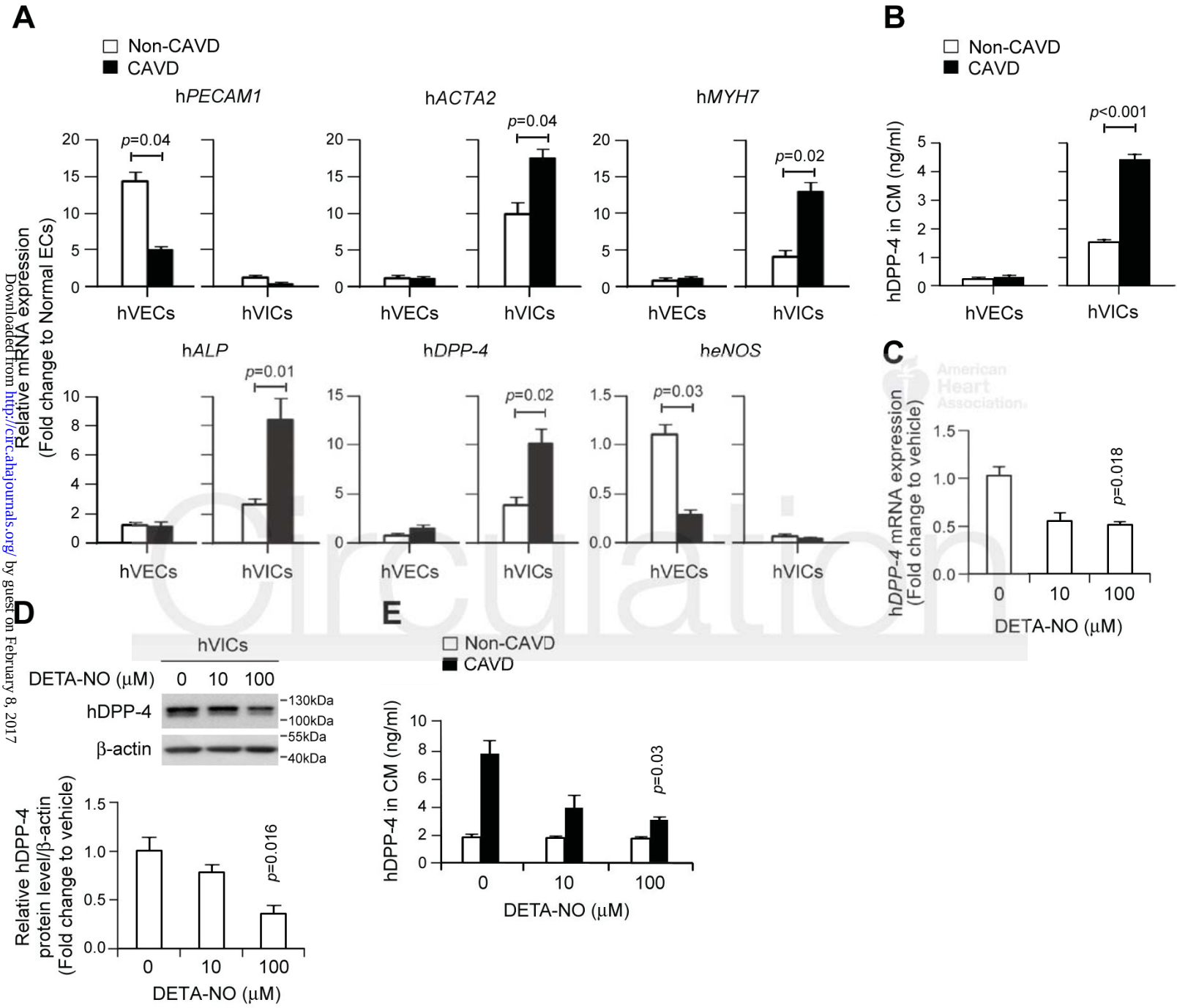

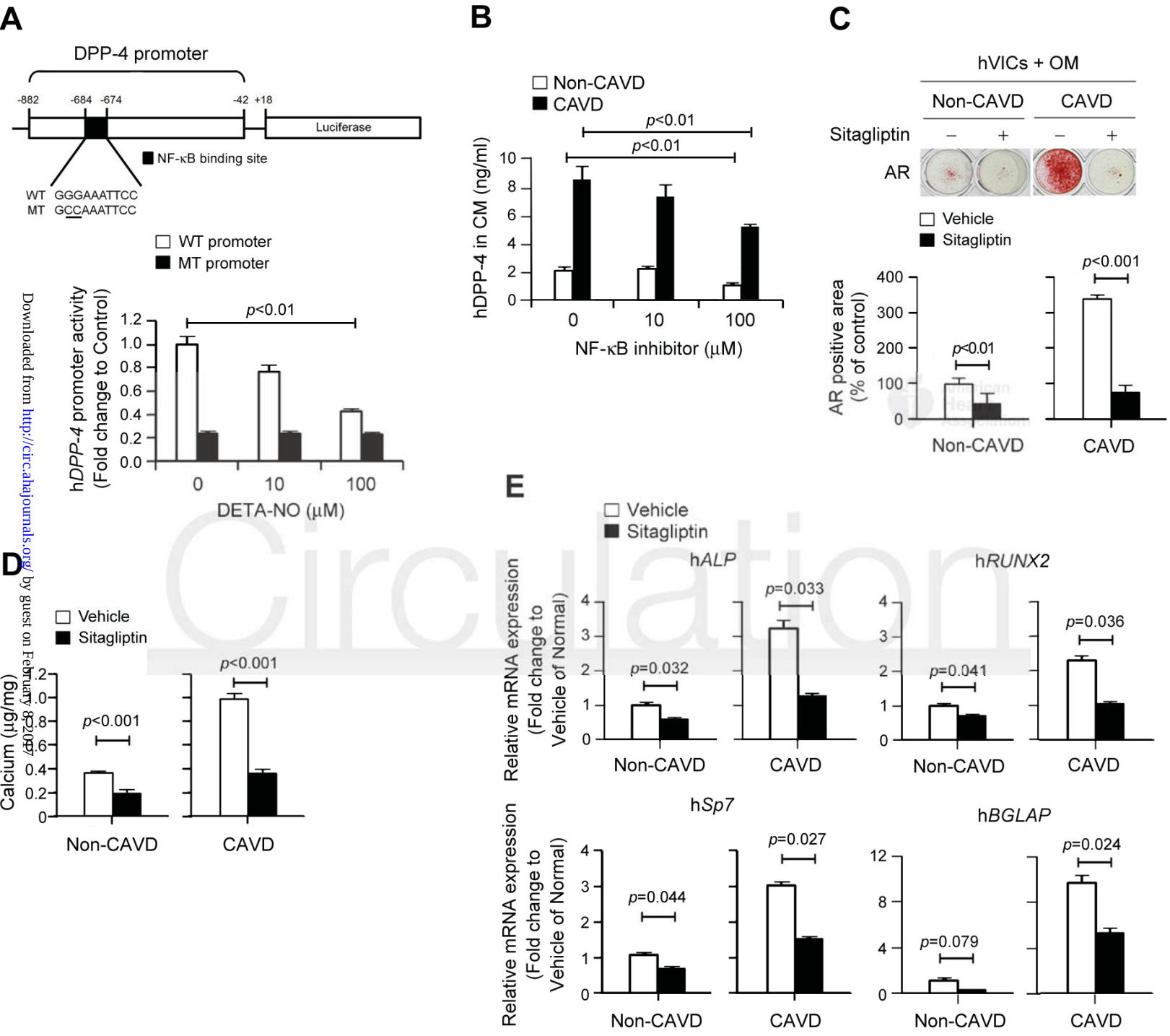

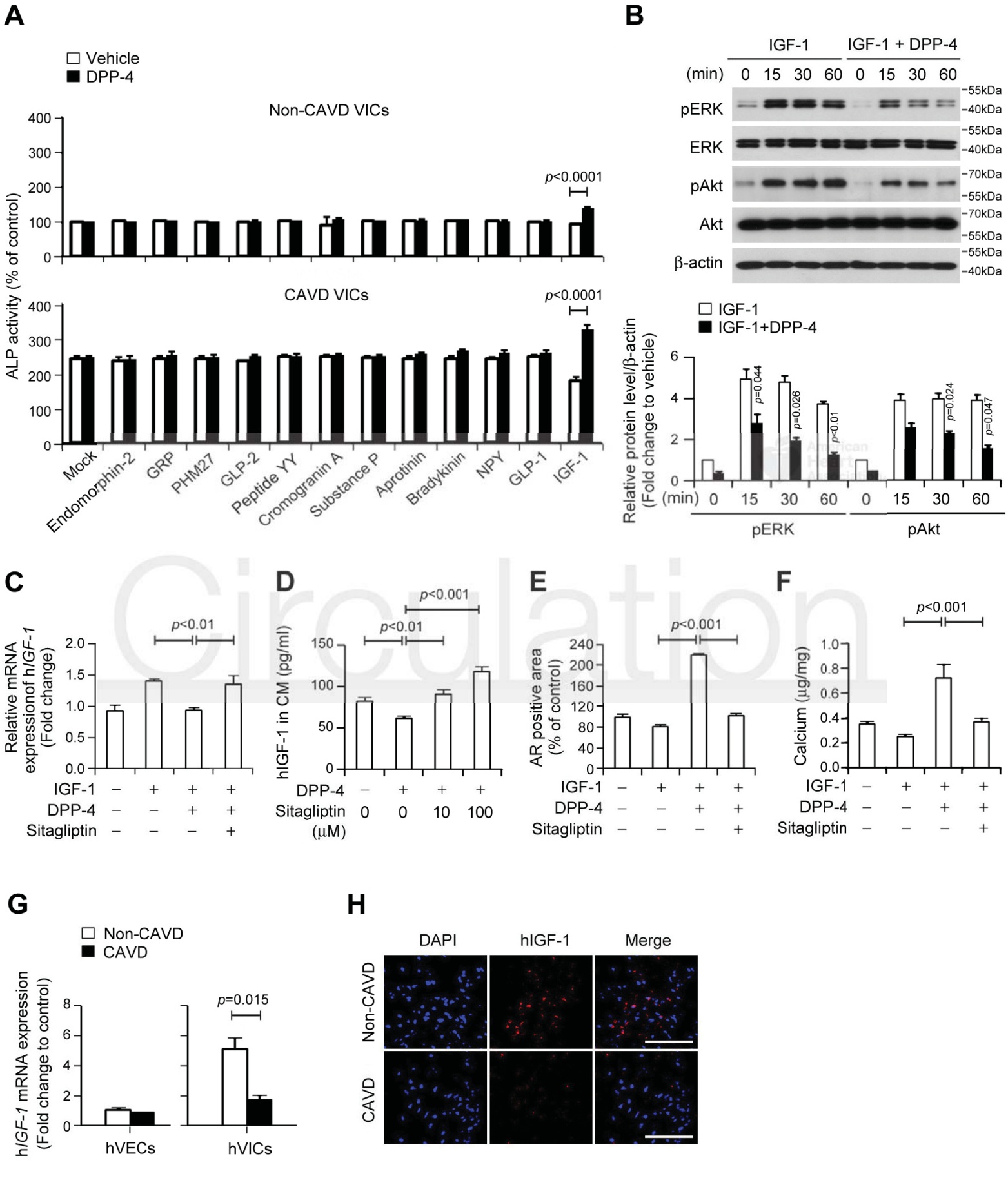

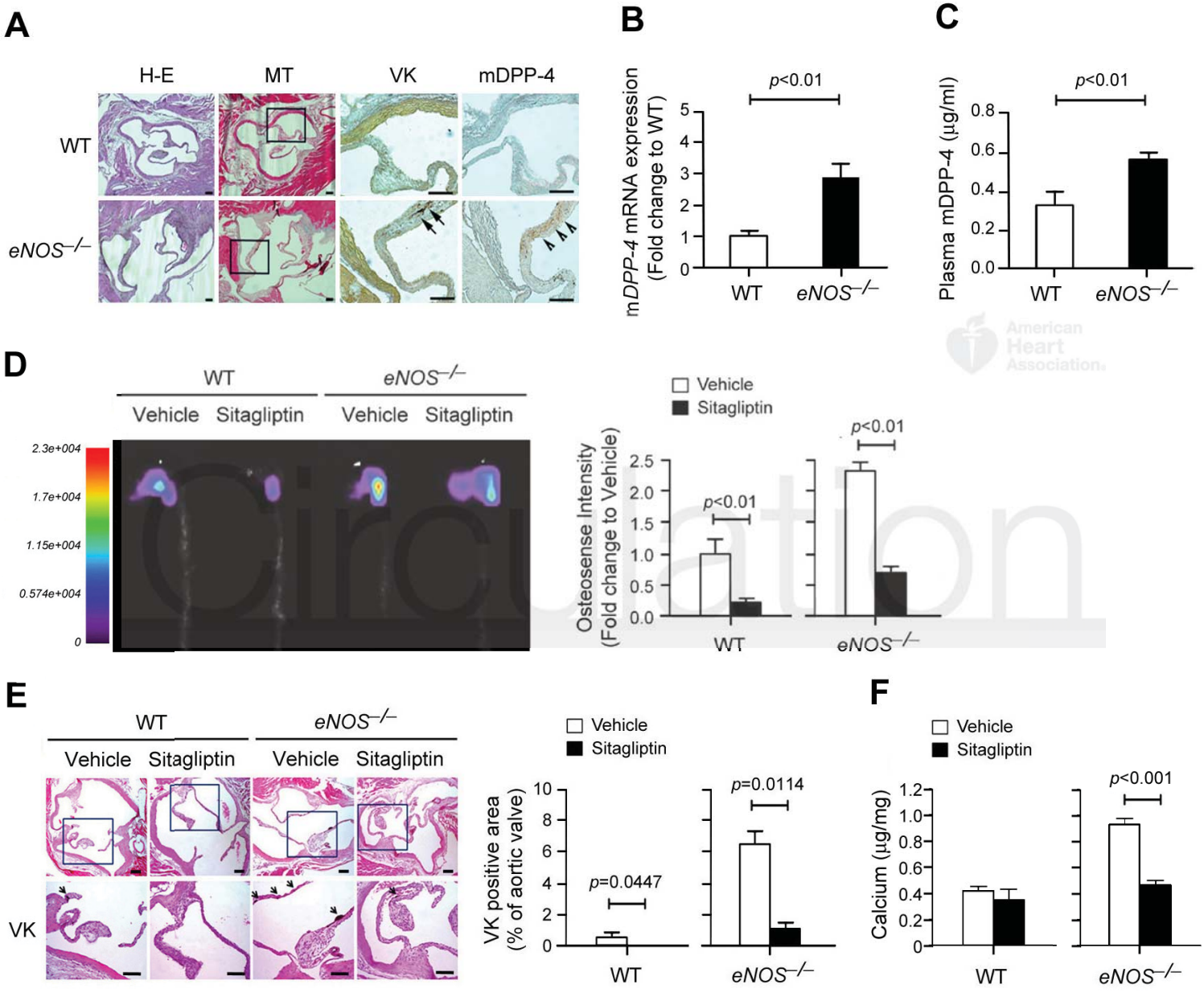

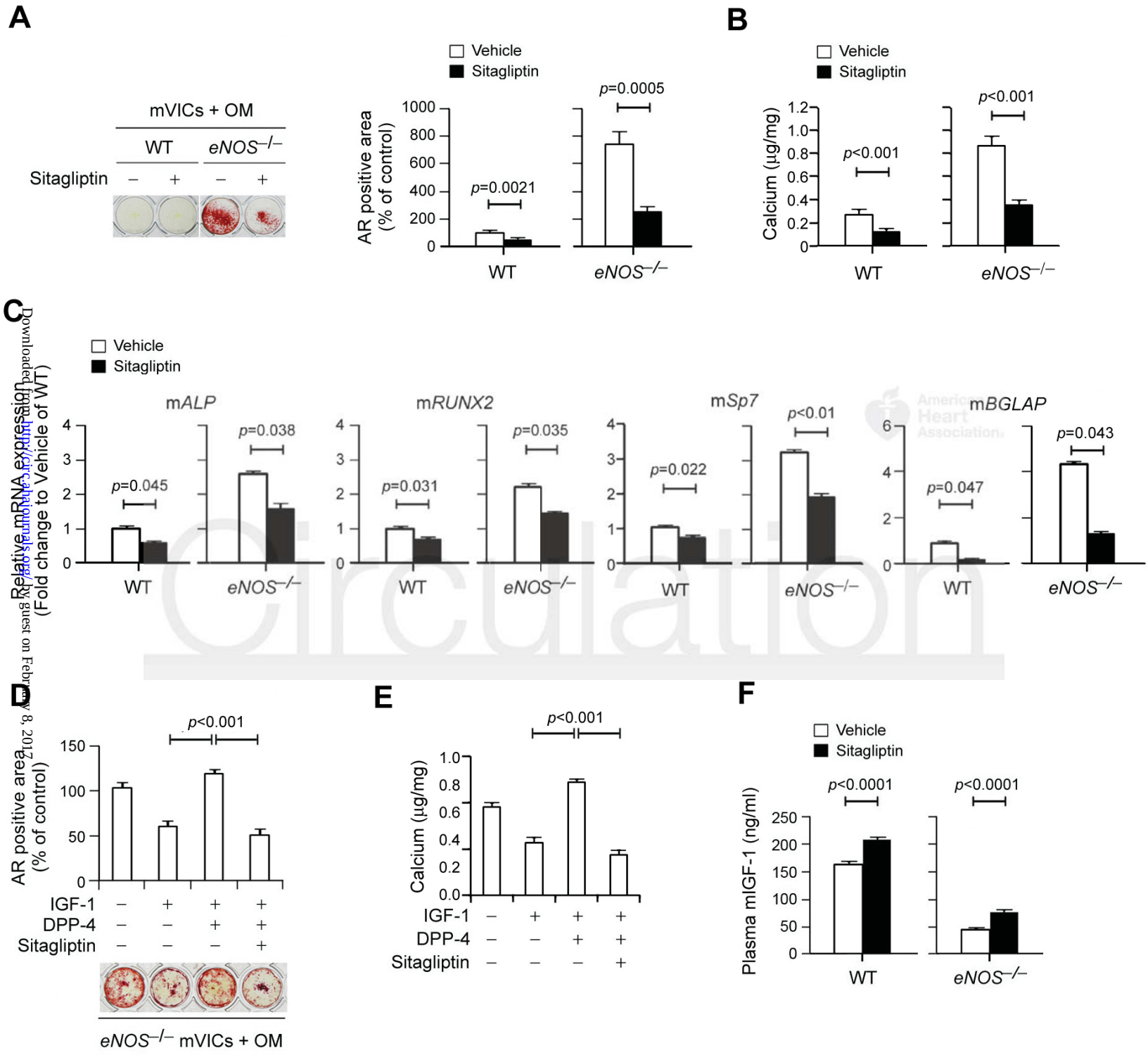

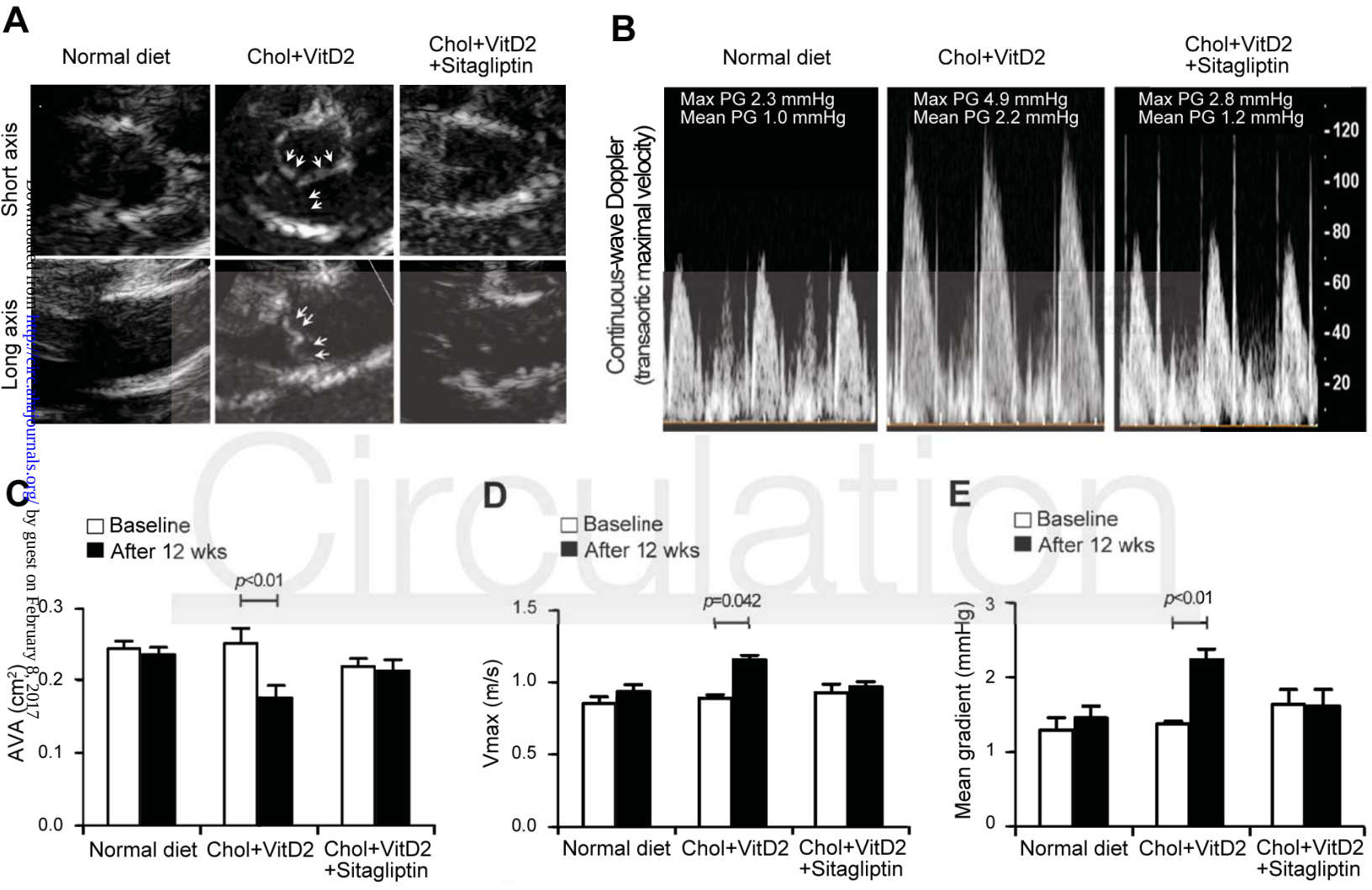

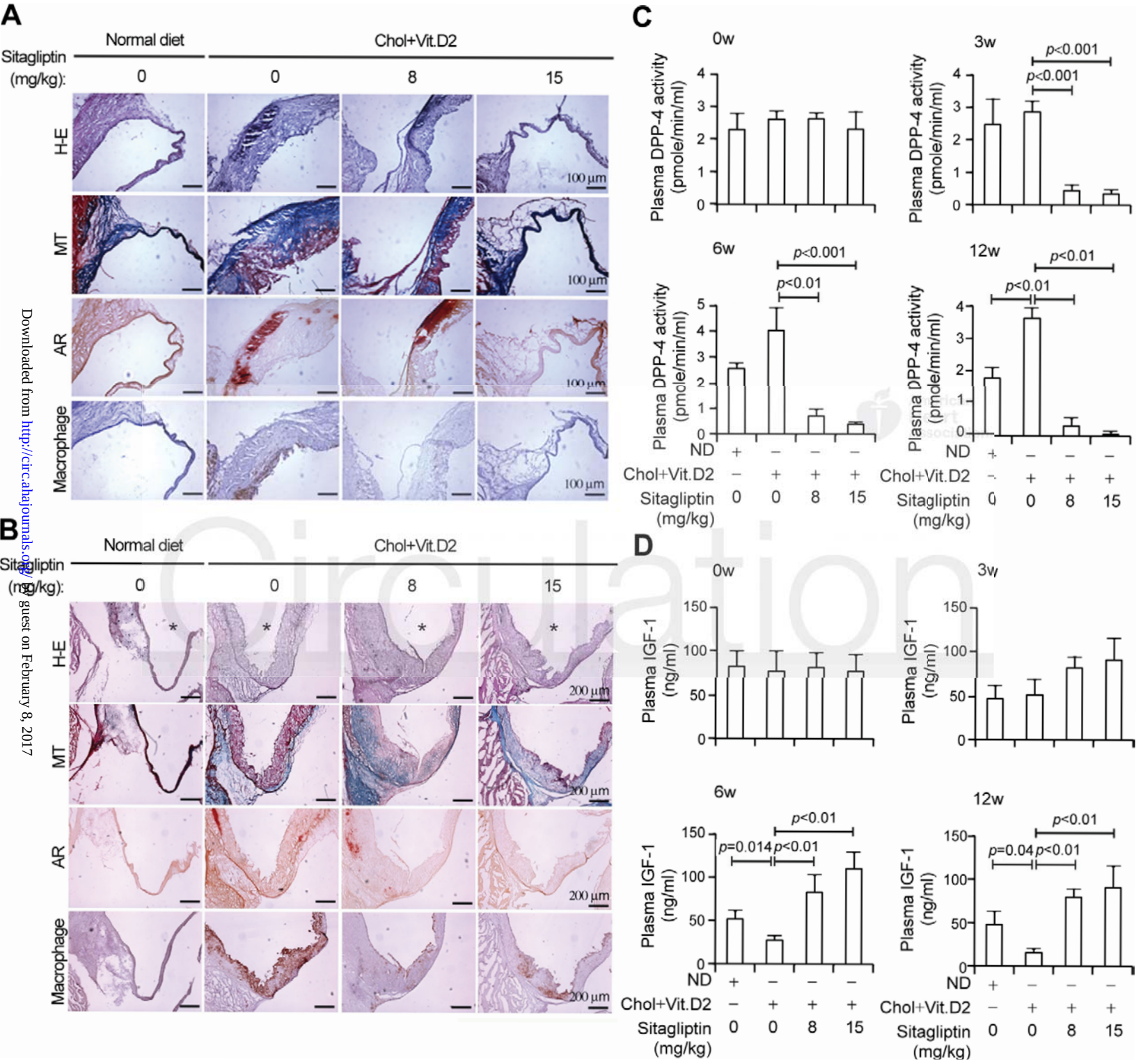

Dipeptidyl Peptidase-4 Induces Aortic Valve Calcification by Inhibiting Insulin-like Growth Factor-1 Signaling in Valvular Interstitial Cells

Bongkun Choi, Sahmin Lee, Sang-Min Kim, Eun-Jin Lee, Sun Ro Lee, Dae-Hee Kim, Jeong Yoon Jang, Sang-Wook Kang, Ki-Up Lee, Eun-Ju Chang and Jae-Kwan Song

Circulation. published online February 8, 2017;
Circulation is published by the American Heart Association, 7272 Greenville Avenue, Dallas, TX 75231

Print ISSN: 0009-7322. Online ISSN: 1524-4539

SUPPLEMENTAL MATERIAL

Online-only Data Supplement for the following *Circulation* article

TITLE: Dipeptidyl Peptidase-4 (DPP-4) Induces Aortic Valve Calcification by Inhibiting Insulin-like Growth Factor-1 Signaling in Valvular Interstitial Cells

AUTHORS: Bongkun Choi, PhD; Sahmin Lee, MD, PhD; Sang-Min Kim, MS; Eun-Jin Lee, PhD; Sun Ro Lee, BS; Dae-Hee Kim, MD, PhD; Jeong Yoon Jang, MD; Sang-Wook Kang, PhD; Ki-Up Lee, MD; Eun-Ju Chang, PhD; Jae-Kwan Song, MD, PhD

Supplemental Methods

Global Gene Expression Analysis

Expression studies of aortic valve specimens of calcific aortic valve disease (CAVD) human patients and non-CAVD human controls were performed using Affymetrix GeneChip® Human Gene 2.0 ST Arrays (Affymetrix). Quantile normalization and analysis of the raw data were performed using Affymetrix GCOS software (Affymetrix). The complete data set is available with NCBI GEO accession number GSE7728.

Cell Culture

Human valvular endothelial cells (VECs), human valvular interstitial cells (VICs), and murine VICs were prepared from aortic valve leaflets and maintained as previously described[1, 2]. VICs

were isolated from the human or murine aortic valve leaflets by enzyme isolation and were grown in Dulbecco's Modified Eagle's Medium (DMEM, Thermo Scientific) supplemented with 10% fetal bovine serum (Thermo Scientific), penicillin (100 U ml^{-1}, Life Technologies), and streptomycin sulfate (Life Technologies), as previously described[3]. VECs were grown in DMEM complete medium supplemented with a EC growth supplement (0.1 mg ml^{-1}, BD Biosciences). Cells at passage 2 to 10 were used for experiments, and induction of calcification of VICs was performed as previously described[4]. Cells were cultured with NO donor DETA-NONOate (Enzo Life Sciences), IGF-1 (R&D), DPP-4 (R&D), NF-κB activation inhibitor (Calbiochem), NF-κB transcriptional activation inhibitor (6-Amino-4-(4-phenoxyphenylethylamino)quinazoline, Calbiochem), or Sitagliptin at the indicated concentrations[5].

Osteogenic Differentiation

Osteogenic differentiation of primary murine VICs isolated from the aortic valves of WT, *eNOS*$^{-/-}$, and *DPP-4*$^{-/-}$ mice was induced in osteogenic media (minimum essential medium α (α-MEM, Thermo Scientific) supplemented with 0.25 mM L-ascorbic acid (Sigma) and 10 mM β-glycerophosphate (Sigma)) for the indicated times.[6] *DPP-4*$^{-/-}$mice were obtained from Institut National de la Sante st la Recherche Medicale (France). To induce osteogenic differentiation of primary human VICs, 0.25 mM L-ascorbic acid, 10 mM β-glycerophosphate, and 10 nM dexamethasone were added to complete medium (DMEM, Thermo Scientific) as previously described.[1] Osteogenic medium was changed every 3 days.

Alkaline phosphatase (ALP), Alizarin red (AR), and Von Kossa (VK) Staining

Osteogenic transdifferentiation and calcification was determined by ALP, AR, and VK staining as previously described.[7] ALP staining was performed using an Alkaline Phosphatase Kit (Sigma) according to the manufacturer's instructions. For AR staining, cells were washed three times with PBS, fixed with 4% formaldehyde for 30 min, washed three times with PBS, and exposed to 2% AR staining (Aqueous, Sigma) for 10 min. For VK staining, cells were incubated with 5% silver nitrate (Amresco) solution for 30 min, exposed to bright sunlight for 1 h, washed, and then treated with 5% sodium thiosulfate (Sigma).

Calcium Assay

Calcium concentration was quantified colorimetrically by the o-cresolphthalein method in 0.1 M HCL extracts from cultured cells or from aortic valve cusp. Calcium content was normalized either to total cellular protein or weight of aortic valve cusp and expressed as microgram calcium per milligram weight. [8]

Reporter Assays

For reporter assays, hVICs or human embryonic kidney (HEK) 293 cells (ATCC) plated on 6-well plates were grown to 80% confluency and then transfected with DPP-4 reporter vectors containing either wildtype (control) or mutated NF-κB binding sites using Lipofectamine 2000 (Life Technologies). Twenty-four hours post-transfection, firefly and *Renilla* luciferase activities were measured using the Dual-Glo Luciferase Assay System (Promega) according to the manufacturer's instructions. Firefly luciferase activity was normalized using *Renilla* luciferase activity. PCR was used to perform site directed mutagenesis at the NF-κB binding site [9] using the following primers: 5'-CCTGCAAGACAATCGCCAAATTCCCTAGGGAG- 3' and 5'-

CTCCCTAGGGAATT TGGC GATTGTCTTGCAGG-3'.

Alkaline Phosphatase (ALP) Activity Assays

ALP activity was determined as previously described [7]. After 1 week of osteogenic stimulation, ALP activity was determined in hVICs treated with the following substrates, which had been incubated either alone or with DPP-4 (50 ng ml^{-1}, R&D): Vehicle (Mock), Endomorphin-2 (R&D), GRP (Gastrin-releasing peptide, R&D), PHM27 (peptide histidine methionine 27, R&D), GLP-2 (Glucagon-like peptide-2, R&D), Peptide YY (R&D), Chromogranin A (Sigma), Substance P (R&D), Aprotinin (Sigma), Bradykinin (Sigma), NPY (neuropeptide-Y, R&D), GLP-1 (Glucagon-like peptide-1, R&D), or IGF-1 (insulin-like growth factor-1, R&D) (each at 200 ng ml-1). ALP activity was also determined in DPP-4 knockout mouse mVICs after 1 week of osteogenic stimulation.

Fluorescence Reflectance Imaging *in vivo*

Bisphosphonate-conjugated imaging agent (Osteosense680, VisEn Medical Inc.) was injected into tail veins of mice to detect osteogenic activity [10, 11]. Osteosense680 binds to sites of calcification *in vivo*, particularly to hydroxyapatite, and serves as an imaging agent for the detection of osteoblastic activity. Mice were euthanized, and the heart and aorta was dissected and imaged with OptixMX3 (ART Advanced Research Technologies Inc.).

Immunohistochemistry

Serial 5-μm paraffin-embedded or frozen cross sections were incubated with anti-DPP-4 antibody (Abcam) or rabbit anti-macrophage antibody (Dako) and developed using the Dako

REAL™ EnVision™ Detection System Peroxidase/DAB+ kit (Dako) according to the manufacturer's instructions. Hematoxylin /eosin (H/E) and masson's trichrome (MT) stains were performed according to manufacturer's instructions (Sigma).

Immunofluorescence staining

For immunofluorescence staining, Alexa Fluor 647 or Cy3-conjugated secondary antibodies were used after an overnight incubation of the lesions with the primary antibodies: anti-DPP-4, anti-alpha-smooth muscle actin (α-SMA) (Abcam), anti-*eNOS* (Abcam), or anti-IGF-1 (Mybioscience) antibody. 4',6-diamidino-2-phenylindole (DAPI) was used for counterstaining. Nonspecific primary antibodies were used as negative controls. Digital images were acquired using a confocal laser-scanning microscope (LSM 710, Carl Zeiss).

RT-PCR and Quantitative Real-Time Polymerase Chain Reaction (qRT-PCR)

Total RNA extraction, RT-PCR, and qRT-PCR were performed as previously described.[6] Briefly, total RNA was isolated using a RNeasy Lipid Tissue kit (Qiagen) according to the manufacturer's instructions. cDNA was synthesized using the RevertAid First strand cDNA Synthesis kit (Thermo Scientific, EU) and PCR was performed in a BIO-RAD T100™-Thermal Cycler. qRT-PCR analysis was conducted in optical 96-well plates using the *Power* SYBR Green *1-Step* kit and an ABI 7000 Real Time PCR System (Applied Biosystems) according to the manufacturer's instructions. Gene expression was normalized to that of *GAPDH*, which was used as an internal control.

Immunoblot Assays

Equal amounts of total protein per sample were subjected to sodium dodecyl sulfate polyacrylamide gel electrophoresis (SDS-PAGE) and western blot analysis as described previously.[12] Cell lysates were resolved on SDS-PAGE gels and then transferred to polyvinylidene difluoride membranes. Proteins were detected using rabbit polyclonal antibodies against DPP-4 (Abcam), pERK, ERK, pAkt, Akt (Cell Signaling Technology), and β-actin (Sigma). Protein bands were visualized using an enhanced chemiluminescence detection system (Pierce).

Enzyme-linked immunosorbent assays (ELISAs)

Plasma concentrations of DPP-4 (R & D) and IGF-1 (R & D) were measured in patients admitted to Asan Medical Center (Seoul, Korea) using an ELISA according to the manufacturer's instructions. A total of 141 patients with or without calcified lesion formation were recruited with written informed consent. The levels of DPP-4 (R&D), IGF-1 (R&D) in plasma from mice, and rabbit IGF-1 (MyBioSource) were also measured using ELISA according to the manufacturer's instructions. Absorbance at 450 nm was measured using a microtiter plate reader (Bio-Rad).

Determination of DPP-4 Activity

DPP-4 activity in human plasma was determined using a DPP-4 activity assay kit (Calbiochem) according to manufacturer's instructions.

Echocardiography

Echocardiography of CAVD rabbit model was performed at baseline and every 3 weeks after the beginning of treatment. Rabbits were anesthetized with an intramuscular injection of using

ketamine (30 mg/kg) and xylazine (6 mg/kg). Aortic valve area and transvalvular gradient were measured as described previously.[13] Both parasternal long axis view and parasternal short axis view were used to observe leaflet morphology and opening of aortic valve. Aortic valve area was measured by the standard continuity equation. The diameter of the left ventricular outflow tract was measured in parasternal long axis view. The stroke volume with pulsed-Doppler proximal to the aortic valve was measured in an apical five chamber view as is routinely done in humans. In addition, continuous-wave Doppler was obtained to measure the integral of transvalvular flow to be used in the continuity equation for aortic valve area calculation, as well as to record maximal and mean trans-aortic pressure gradients.

Supplemental Tables

Supplementary Table 1. Characteristics of non-CAVD cardiac transplant recipients

	non-CAVD cardiac transplant recipients (*n*=8)
Age, y*	49 ± 17
Male, n†	6 (75)
Heart disease	
Dilated cardiomyopathy	6 (75)
Ischemic cardiomyopathy	1 (12.5)
Others (i.e. chronic rejection)	1 (12.5)
Height, cm	166 ± 9.6
Weight, kg	63 ± 13.8
Body surface area, m^2	1.7 ± 0.2
Body mass index, kg/m^2	23.0 ± 4.2
Left ventricular diastolic dimension, mm	70 ± 8.2
Left ventricular ejection fraction, %	26 ± 11.3
Transaortic peak velocity, m/s	1.0 ± 0.3
Hypertension, n	1 (12.5)
Diabetes, n	2 (25)
Dyslipidemia, n	1 (12.5)
Renal insufficiency, n	1 (12.5)
Previous stroke, n	2 (25)

The values are presented as frequencies, percentages, and mean ± standard deviation. Values in parentheses are percentages. * year; †number.

Supplementary Table 2. Changes in Clinical and Echocardiographic Characteristics Over Study Period According to Experimental Rabbit Group

	Control group	Chol + VitD2 group	Sitagliptin group	*p* value
Body weight, kg				
Baseline	2.82 ± 0.39	2.90 ± 0.38	2.91 ±0.32	0.949
12 weeks	3.34 ± 0.10	3.01 ± 0.42	3.01 ± 0.17	0.051
Blood glucose, mg/dl				
Baseline	154.8 ± 8.9	154.8 ± 69.7	154.3 ± 9.1	0.990
12 weeks	153.0 ± 19.6	199.0 ± 10.3	113.7 ± 9.3	0.008
Posterior wall thickness, mm				
Baseline	2.44 ± 0.29	2.40 ± 0.14	2.52 ± 0.22	0.468
12 weeks	2.56 ± 0.09	2.77 ± 0.14	2.68 ± 0.16	0.173
Septum thickness, mm				
Baseline	2.72 ± 0.16	2.54 ± 0.30	2.44 ± 0.27	0.223
12 weeks	2.62 ± 0.13	2.81 ± 0.10	2.92 ± 0.22	0.047
LV * diastolic dimension, mm				
Baseline	11.7 ± 0.51	12.2 ± 1.56	12.0 ± 0.92	0.761
12 weeks	12.6 ± 0.72	13.4 ± 1.49	12.4 ± 1.35	0.610
LV mass, g				
Baseline	3.27 ± 0.41	3.28 ± 0.42	3.22 ± 0.41	0.914
12 weeks	3.62 ± 0.36	4.30 ± 0.55	3.89 ± 0.49	0.131
Aortic valve area, cm^2				
Baseline	0.24 ± 0.02	0.25 ± 0.05	0.22 ± 0.02	0.266
12 weeks	0.25 ± 0.03	0.18 ± 0.04	0.21 ± 0.03	0.037

Maximal transaortic velocity, m/s				
Baseline	0.85 ± 0.11	0.89 ± 0.05	0.94 ± 0.13	0.289
12 weeks	0.94 ± 0.11	1.16 ± 0.07	0.98 ± 0.08	0.020
Maximal gradient, mmHg				
Baseline	3.04 ± 0.74	3.26 ± 0.23	3.74 ± 0.95	0.363
12 weeks	3.20 ± 0.60	5.00 ± 0.68	3.44 ± 1.00	0.014
Mean gradient, mmHg				
Baseline	1.30 ± 0.37	1.38 ± 0.08	1.64 ± 0.45	0.286
12 weeks	1.46 ± 0.36	2.24 ± 0.32	1.62 ± 0.50	0.035
Plasma DPP-4 [†] activity, pmole/min/ml				
Baseline	2.31 ± 0.48	2.62 ± 0.23	2.31 ± 0.54	0.430
12 weeks	1.78 ± 0.31	3.61 ± 0.33	0.24 ± 0.09	0.008
Plasma IGF-1 [‡], ng/mL				
Baseline	82.3 ± 17.6	76.6 ± 22.2	76.2 ± 19.3	0.852
12 weeks	48.2 ± 15.2	16.0 ± 4.6	91.0 ± 24.1	0.010

[*]LV, left ventricle; [†]DPP-4, dipeptidyl peptidase-4; [‡]IGF-1, insulin-like growth factor-1. All statistical analyses were performed using the nonparametric Kruskal-Wallis test. The statistics are presented as mean ± standard deviation. A value of $p<0.05$ was considered significant.

Supplemental Figures

Supplementary Figure 1.

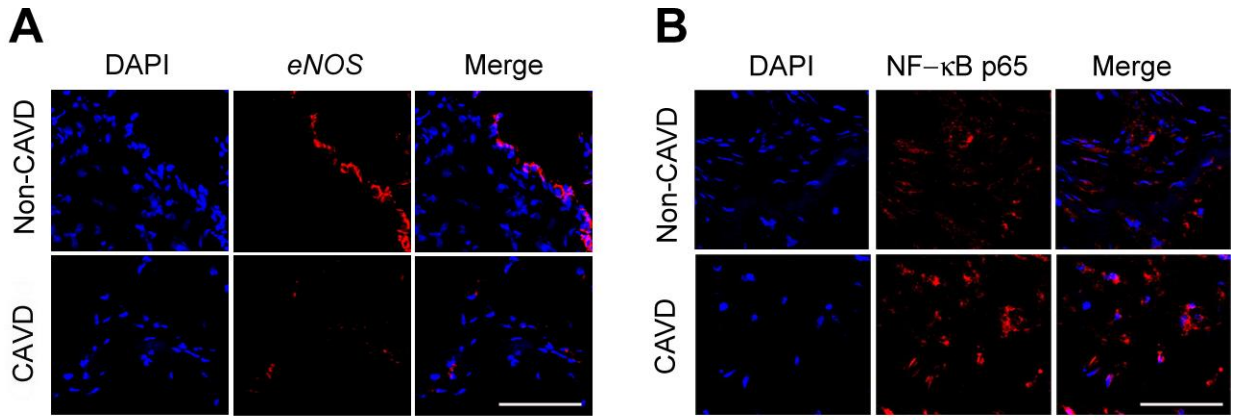

Reduction of eNOS expression and induction of NF-κB expression in aortic valve tissue of CAVD patient

Immunofluorescence staining of eNOS (A) and NF-κB (B) in aortic valve tissues from non-CAVD controls and CAVD patients. For immunofluorescence staining, serial 5-μm cross sections of aortic valve were incubated with anti-eNOS (A) and anti-NF-κB (B) antibodies. Alexa Fluor 647-conjugated secondary antibody was applied for visualization after an overnight incubation of the lesions with the primary antibody. Nuclei were stained with 4’,6-diamidino-2-phenylindole (DAPI, blue). Digital images were acquired using a confocal laser-scanning microscope. Scale bar, 100 μm.

Supplementary Figure 2.

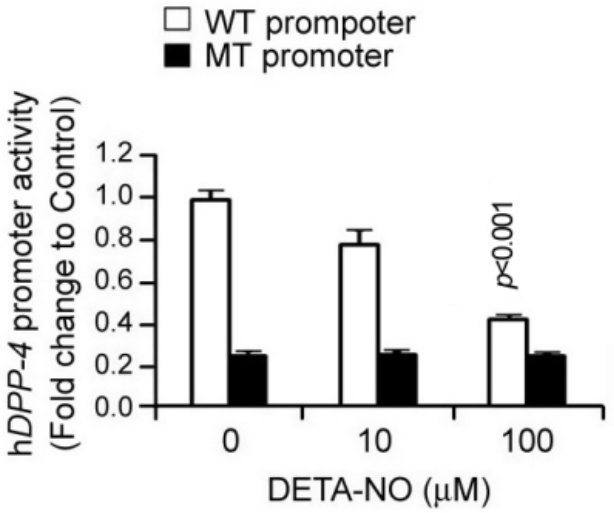

h*DPP-4* promoter activity which was measured in HEK293 cells after transfection with either the luciferase constructs of the wild-type (WT) or mutations (MT) h*DPP-4* promoters followed by treatment with DETA-NO.

Supplementary Figure 3.

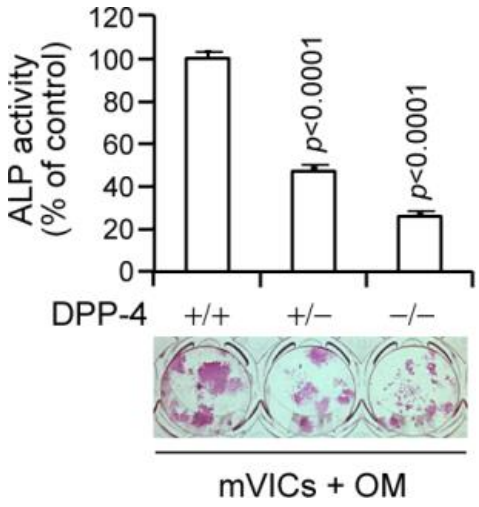

Attenuation of *in vitro* calcification associated with down-regulation of DPP-4

Alkaline phosphatase (ALP) activity (upper panel) was determined and ALP staining (lower panel) was performed in wild-type and DPP-4 knockout mVICs after 1 week of osteogenic stimulation (OM). The bar graph presents the ALP activity measured in each culture dish. Data represent the mean±standard deviation. *p* values were obtained using Student's *t* tests.

Supplementary Figure 4.

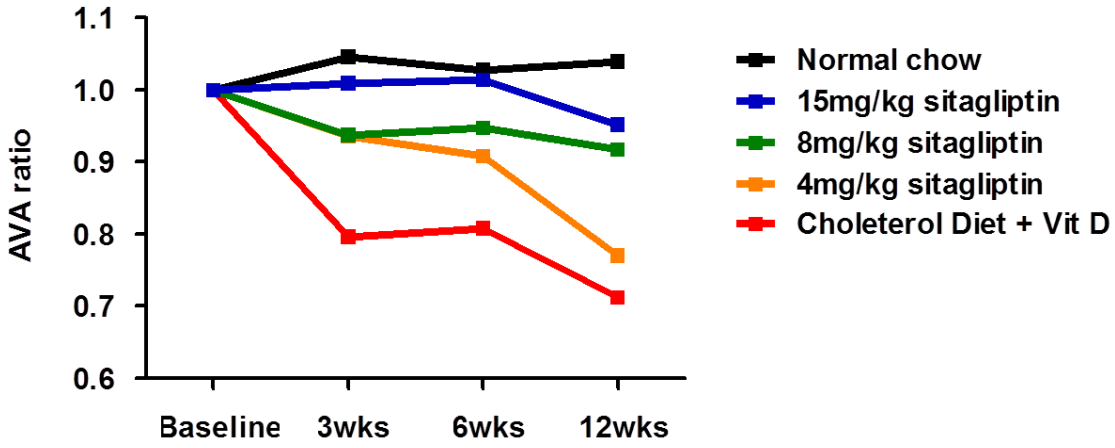

Alterations in aortic valve area of rabbits treated with different doses of Sitagliptin

In animal study using a rabbit CAVD model induced by high cholesterol diet with vitamin D2 supplementation, rabbits were given Sitagliptin orally at doses of 4, 8 or 15 mg/kg per day to determine the most effective dosage for attenuating aortic valve stenosis. The results were expressed as the ratio of aortic valve area (AVA) measured at the time of 3, 6, or 12 weeks to the AVA at baseline in each group. There were at least five animals in each group.

Supplementary Figure 5.

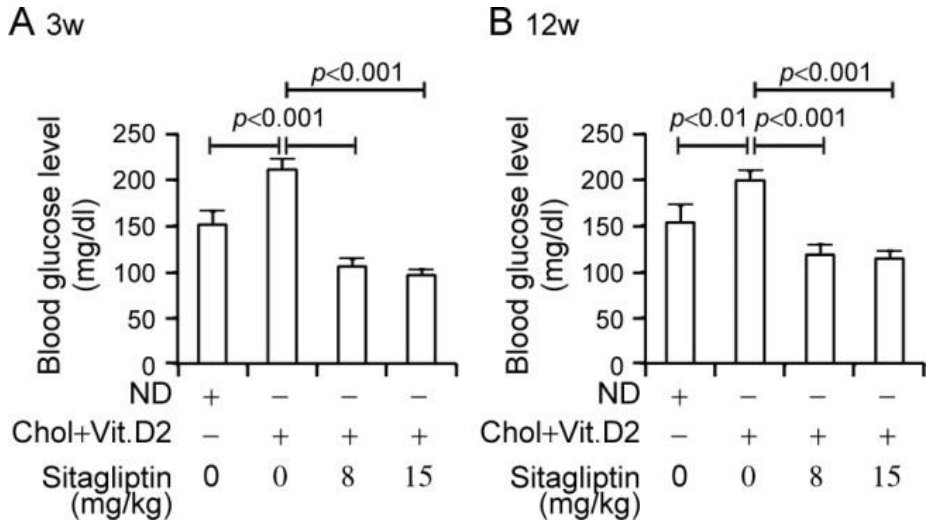

Blood glucose levels in rabbits challenged with high dose Sitagliptin

The levels of blood glucose were measured in rabbits at 3 weeks (A) and at 12 weeks (B). Even in rabbits treated with high dose Sitagliptin (8 or 15 mg/kg), the glucose levels remained within the normal rage without any evidence of hypoglycemia. Data represent the mean±standard deviation. *p* values were obtained using Student's *t* tests.

Supplementary Figure 6.

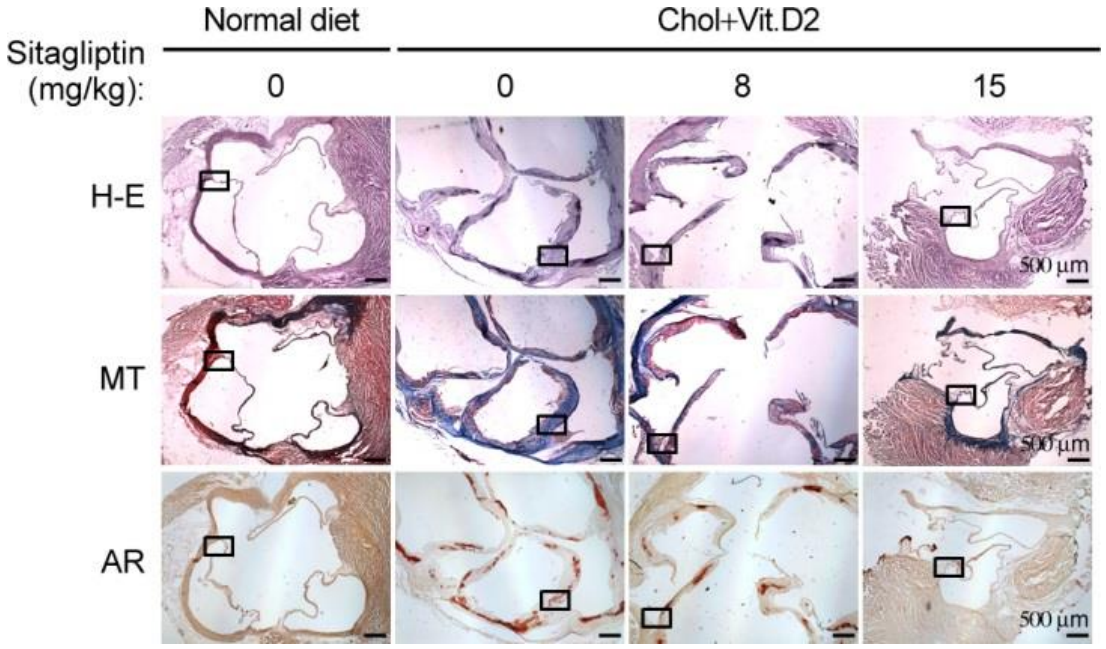

Low-magnification view of cross-sectional images of rabbit aortic valves

Aortic valves from rabbits fed high cholesterol and vitamin D2 supplements (Chol+Vit.D2) are characterized by increased valve thickness (H-E) and cellularity (MT), and development of calcification nodules (AR). The treatment of Sitagliptin can reverse the leaflet morphology like that in the control group fed normal diet (Normal diet). Figure 8A shows magnified views of *box* in these cross-sectional images.

Supplementary Figure 7.

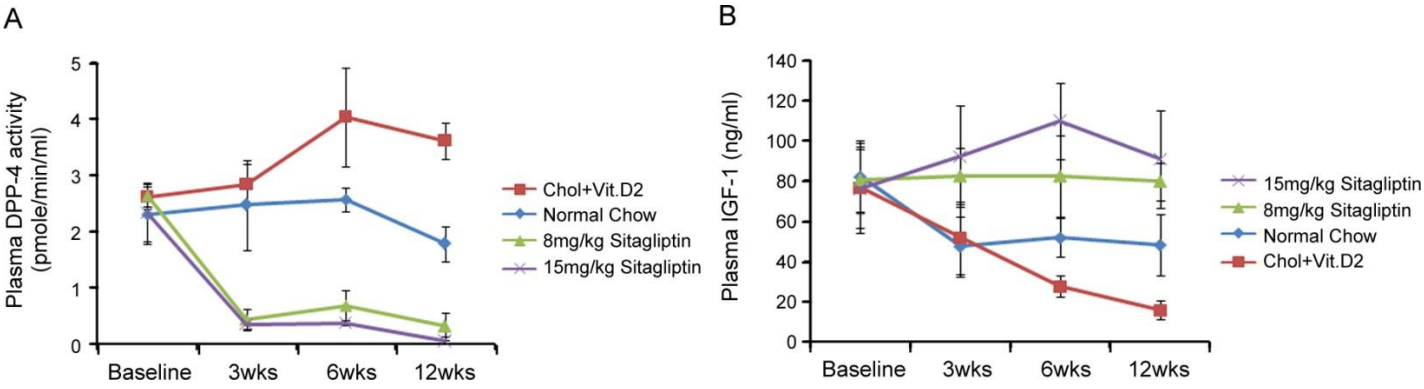

Alterations in plasma DPP-4 activity and IGF-1 level over the 12 week study period.

(A) Plasma DPP-4 activity and (B) IGF-1 levels were measured at baseline and at 3, 6, or 12 weeks in each group. Time-dependent decrease in plasma IGF-1 levels was observed in the cholesterol-vit.D2 group, which was associated with high DPP-4 activities. In contrast, IGF-1 levels remained steady with low DPP-4 activities in the Sitagliptin group over the 12 week study period. Data represent the mean±standard deviation. Statistical analyses were performed using a linear mixed model.

Supplementary Figure 8.

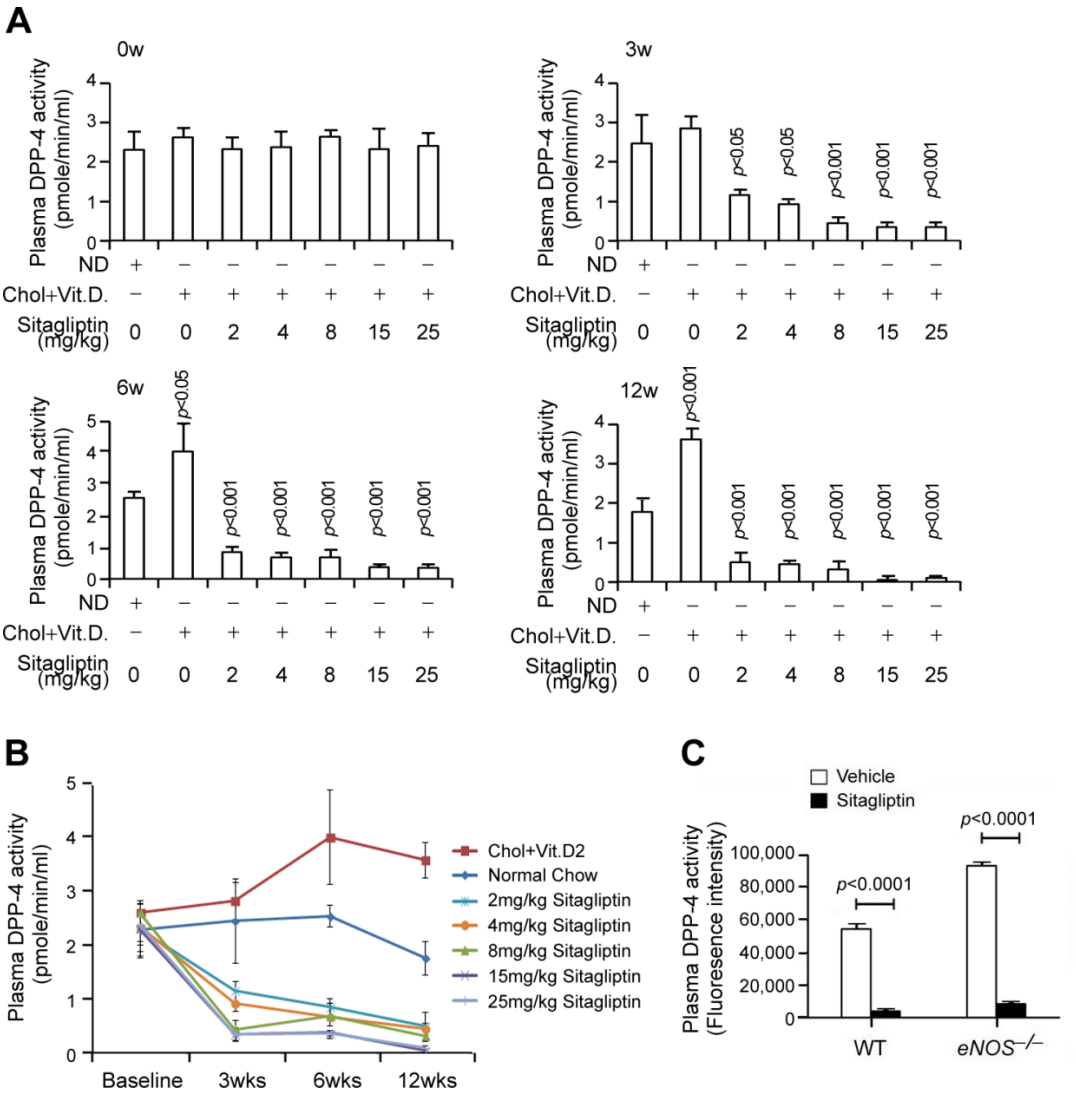

Alterations in DPP-4 activity of animal models treated with sitagliptin (A-B) In a rabbit CAVD model induced by high cholesterol diet with vitamin D2 supplementation, plasma DPP-4 activity in rabbits given Sitagliptin orally at doses of 2, 4, 8, 15 or 25 mg/kg per day was measured to determine the most effective dosage for attenuating aortic valve stenosis. There were at least five animals in each group. (C) The plasma DPP-4 activity in WT and eNOS-/- mice given Sitagliptin orally at doses of 15 mg/kg per day was measured. Data represent the mean±standard deviation.

Supplementary Figure 9.

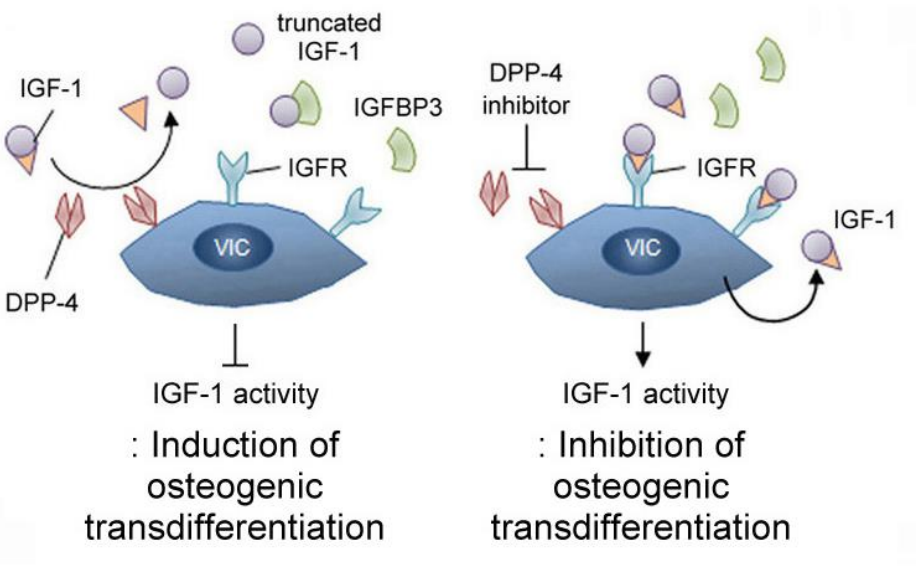

Proposed model of DPP-4 action to promote VIC osteogenic differentiation

DPP-4 cleaves IGF-1, resulting in the induction of VIC osteogenic differentiation via the inhibition of IGF-1-IGFR signaling. Inhibiting DPP-4 prevents VIC osteogenic differentiation by allowing full length IGF-1 to bind to the IGFR and promote IGFR signaling.

Supplementary Figure 10.

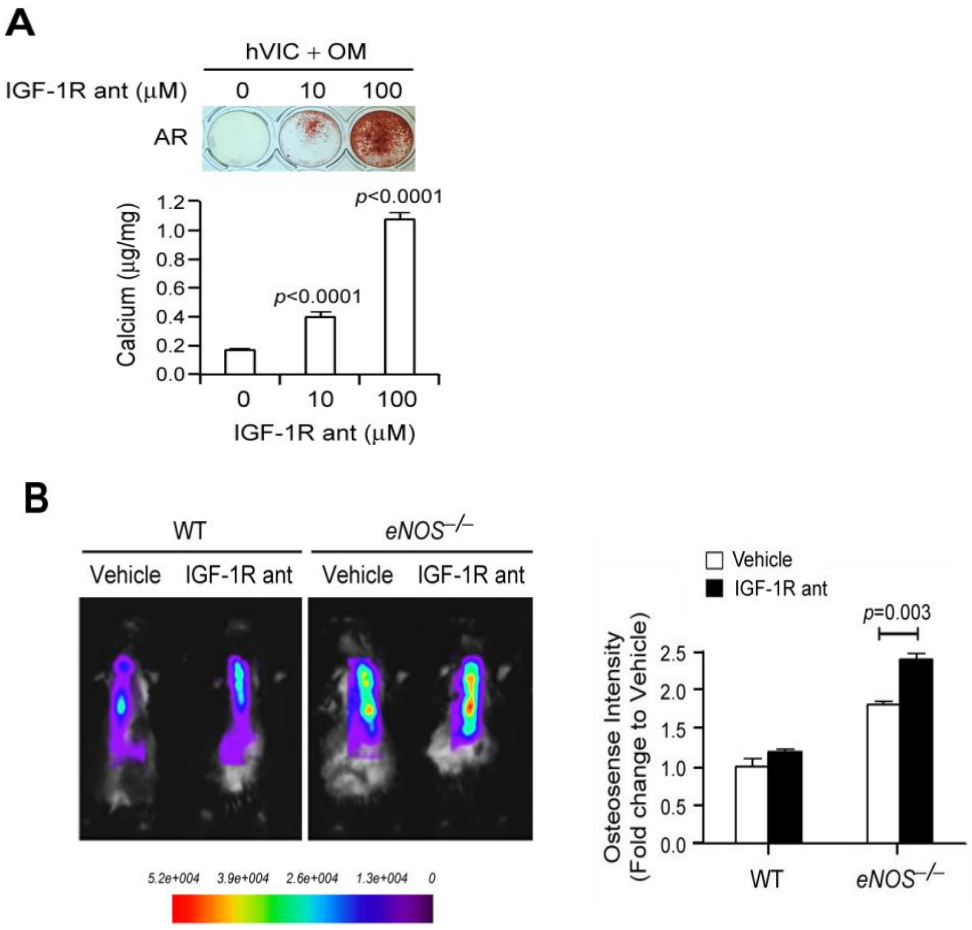

IGF-1 receptor antagonist enhances *in vitro* calcification of hVICs and *in vivo* calcified lesion formation in the aortic valves of eNOS$^{-/-}$ mouse. (A) AR staining of non-CAVD hVICs treated with indicated concentrations of IGF-1 receptor antagonist (IGF-1 R ant, picropodophyllin) after 2 weeks of osteogenic stimulation. (B) Molecular imaging was used to visualize osteogenesis in WT and eNOS$^{-/-}$ mice injected with fluorescent agent (Osteosense680), followed by treatment with vehicle or IGF-1 receptor antagonist (IGF-1 R ant, picropodophyllin, 3 mg/kg/day) for 12 weeks (n = 3 per group). Data represent the mean±standard deviation. *p* values were obtained using Student's *t* tests.

Supplementary Figure 11.

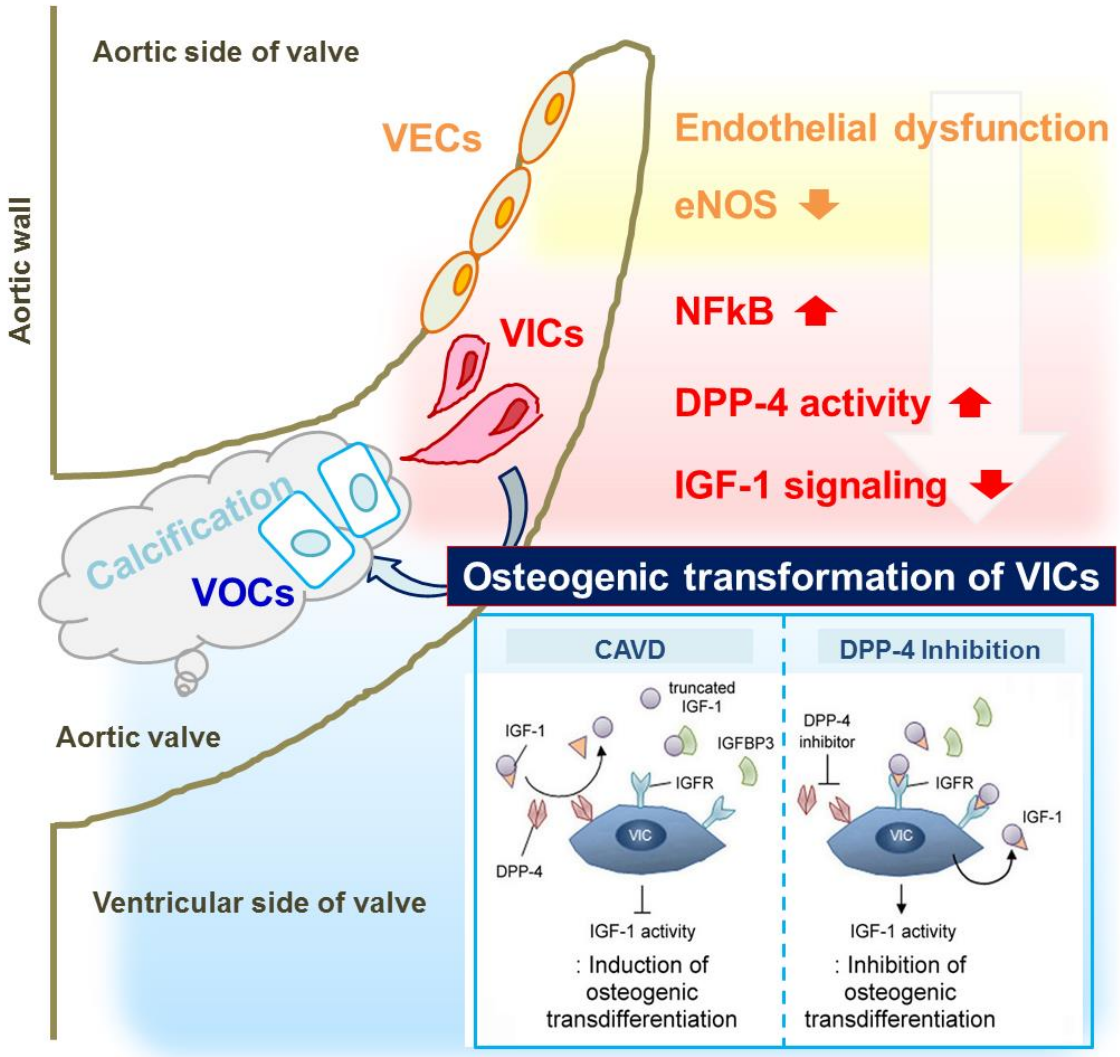

A schematic figure of suggested mechanism of calcific progression of aortic stenosis

The low expression of eNOS in valvular endothelial cells (VECs) induces an alteration of DPP-4 expression via NF-kB activation in valvular interstitial cells (VICs), resulting in the suppression of IGF-1 signaling that leads to the osteogenic transfomarion of VICs to valvular osteoblast-like cells (VOCs). This suggests a new mechanism of calcific aortic valve disease (CAVD).

Supplemental References

1. Loddick SA, Liu XJ, Lu ZX, Liu C, Behan DP, Chalmers DC, Foster AC, Vale WW, Ling N and De Souza EB. Displacement of insulin-like growth factors from their binding proteins as a potential treatment for stroke. *Proc Natl Acad Sci U S A*. 1998;95:1894-1898.

2. Li X, Lim J, Lu J, Pedego TM, Demer L and Tintut Y. Protective Role of Smad6 in Inflammation-Induced Valvular Cell Calcification. *J Cell Biochem*. 2015;116:2354-2364. doi: 10.1002/jcb.25186.

3. Ross R, Glomset J, Kariya B and Harker L. A platelet-dependent serum factor that stimulates the proliferation of arterial smooth muscle cells in vitro. *Proc Natl Acad Sci U S A*. 1974;71:1207-1210.

4. Tintut Y, Parhami F, Bostrom K, Jackson SM and Demer LL. cAMP stimulates osteoblast-like differentiation of calcifying vascular cells. Potential signaling pathway for vascular calcification. *J Biol Chem*. 1998;273:7547-7553.

5. Rees DD, Palmer RM, Schulz R, Hodson HF and Moncada S. Characterization of three inhibitors of endothelial nitric oxide synthase in vitro and in vivo. *Br J Pharmacol*. 1990;101:746-752.

6. Byon CH, Javed A, Dai Q, Kappes JC, Clemens TL, Darley-Usmar VM, McDonald JM and Chen Y. Oxidative stress induces vascular calcification through modulation of the osteogenic transcription factor Runx2 by AKT signaling. *J Biol Chem*. 2008;283:15319-15327. doi: 10.1074/jbc.M800021200.

7. Du Y, Gao C, Liu Z, Wang L, Liu B, He F, Zhang T, Wang Y, Wang X, Xu M, Luo GZ, Zhu Y, Xu Q, Wang X and Kong W. Upregulation of a disintegrin and metalloproteinase with thrombospondin motifs-7 by miR-29 repression mediates vascular smooth muscle calcification.

Arterioscler Tthromb Vasc Biol. 2012;32:2580-2588. doi: 10.1161/ATVBAHA.112.300206.

8. Beazley KE, Eghtesad S and Nurminskaya MV. Quercetin attenuates warfarin-induced vascular calcification in vitro independently from matrix Gla protein. *J Biol Chem*. 2013;288:2632-2640. doi: 10.1074/jbc.M112.368639.

9. Chang JH, Xiao Y, Hu H, Jin J, Yu J, Zhou X, Wu X, Johnson HM, Akira S, Pasparakis M, Cheng X and Sun SC. Ubc13 maintains the suppressive function of regulatory T cells and prevents their conversion into effector-like T cells. *Nat Immunol*. 2012;13:481-490. doi: 10.1038/ni.2267.

10. Aikawa E, Nahrendorf M, Figueiredo JL, Swirski FK, Shtatland T, Kohler RH, Jaffer FA, Aikawa M and Weissleder R. Osteogenesis associates with inflammation in early-stage atherosclerosis evaluated by molecular imaging in vivo. *Circulation*. 2007;116:2841-2850.

11. Zaheer A, Lenkinski RE, Mahmood A, Jones AG, Cantley LC and Frangioni JV. In vivo near-infrared fluorescence imaging of osteoblastic activity. *Nat Biotechnol*. 2001;19:1148-1154.

12. Chung YH, Jang Y, Choi B, Song DH, Lee EJ, Kim SM, Song Y, Kang SW, Yoon SY and Chang EJ. Beclin-1 Is Required for RANKL-Induced Osteoclast Differentiation. *J Cell Physiol*. 2014;229:1963-1971. doi: 10.1002/jcp.24646.

13. Kamimura R, Suzuki S, Sakamoto H, Miura N, Misumi K and Miyahara K. Development of atherosclerotic lesions in cholesterol-loaded rabbits. *Exp Anim.* 1999;48:1-7.